Acta Geologica Polonica, Vol. 71 (2021), No. 3, pp. 305–344
DOI: 10.24425/agp.2020.134559

A putative Tournaisian and Visean volcanic-sedimentary succession in the Lublin Basin, SE Poland: depositional processes, petrological characteristics and sequence stratigraphy

MARIA I. WAKSMUNDZKA*, ALEKSANDRA KOZŁOWSKA and MAGDALENA PAŃCZYK

Polish Geological Institute – National Research Institute, Rakowiecka 4, PL-00-975 Warsaw, Poland.
** Corresponding author; e-mail: maria.waksmundzka@pgi.gov.pl*

ABSTRACT:

Waksmundzka, M.I., Kozłowska, A. and Pańczyk, M. 2021. A putative Tournaisian and Visean volcanic-sedimentary succession in the Lublin Basin, SE Poland: depositional processes, petrological characteristics and sequence stratigraphy. *Acta Geologica Polonica*, **71** (3), 305–344. Warszawa.

The aim of this study was to establish the stratigraphic extent of a putative Tournaisian Stage within the Carboniferous succession in the Lublin Basin. The oldest part of the succession, known as the Huczwa Formation and comprising depositional sequences 1–4, was investigated based on lithofacies analysis, sequence stratigraphy and petrographic studies. The article provides descriptions of depositional sequences, parasequences (cyclothems) and lithofacies that were formed in a range of environments (elements of depositional architecture) and as a result of volcanic processes – lava and pyroclastic eruptions and chemical weathering of their products. Correlation of the sequence stratigraphy to the West European and global Carboniferous chronostratigraphic divisions, as well as to the Khoriv suite in the Lviv-Volyn Basin in adjacent Ukraine, indicates a putative late Tournaisian age for sequence 1, and a late Visean age for sequences 2–4. There is a stratigraphic gap between sequences 1 and 2, spanning probably the uppermost Tournaisian and the lower and middle Visean. The upper Tournaisian is represented by the FRST-LST deposits of sequence 1, comprising mainly volcaniclastic conglomerates and sandstones developed in braided-river channels and incised valleys with hyperconcentrated flow processes. These deposits are represented by polymictic paraconglomerate and lithic/sublithic/subarkose arenites or sublithic wackes, and contain predominantly grains of acidic and alkaline volcanic and igneous rocks. This material probably came from the Łuków-Wisznice Elevation and the Volynian Polesia region, located to the NE and E of the Lublin Basin. In the uppermost part of sequence 1, volcanic rocks and tuffs appear which developed during the activity of at least three volcanic cones in the Lublin Basin. The volcanoes were the source of alkaline lavas in the central and SW areas of the basin, and of acidic lavas in the SE area, previously undescribed. The Visean sequences 2–4 consist of the FRST-LST sediments deposited within incised valleys. The TST and HST deposits accumulated mainly in a shallow ramp-type carbonate shelf, shallow clayey shelf and deltaic environments.

Key words: Tournaisian; Visean; Lublin Basin; Sequence stratigraphy; Petrography; Cyclothems; Volcanic source areas.

INTRODUCTION

The aim of this study is to establish the occurrence and stratigraphic extent of presumed Tournaisian–Visean deposits within the Carboniferous section in the Lublin Basin (Text-fig. 1), undefined to date. The oldest part of the Carboniferous succession, distinguished as the Kłodnica Member (lower part of

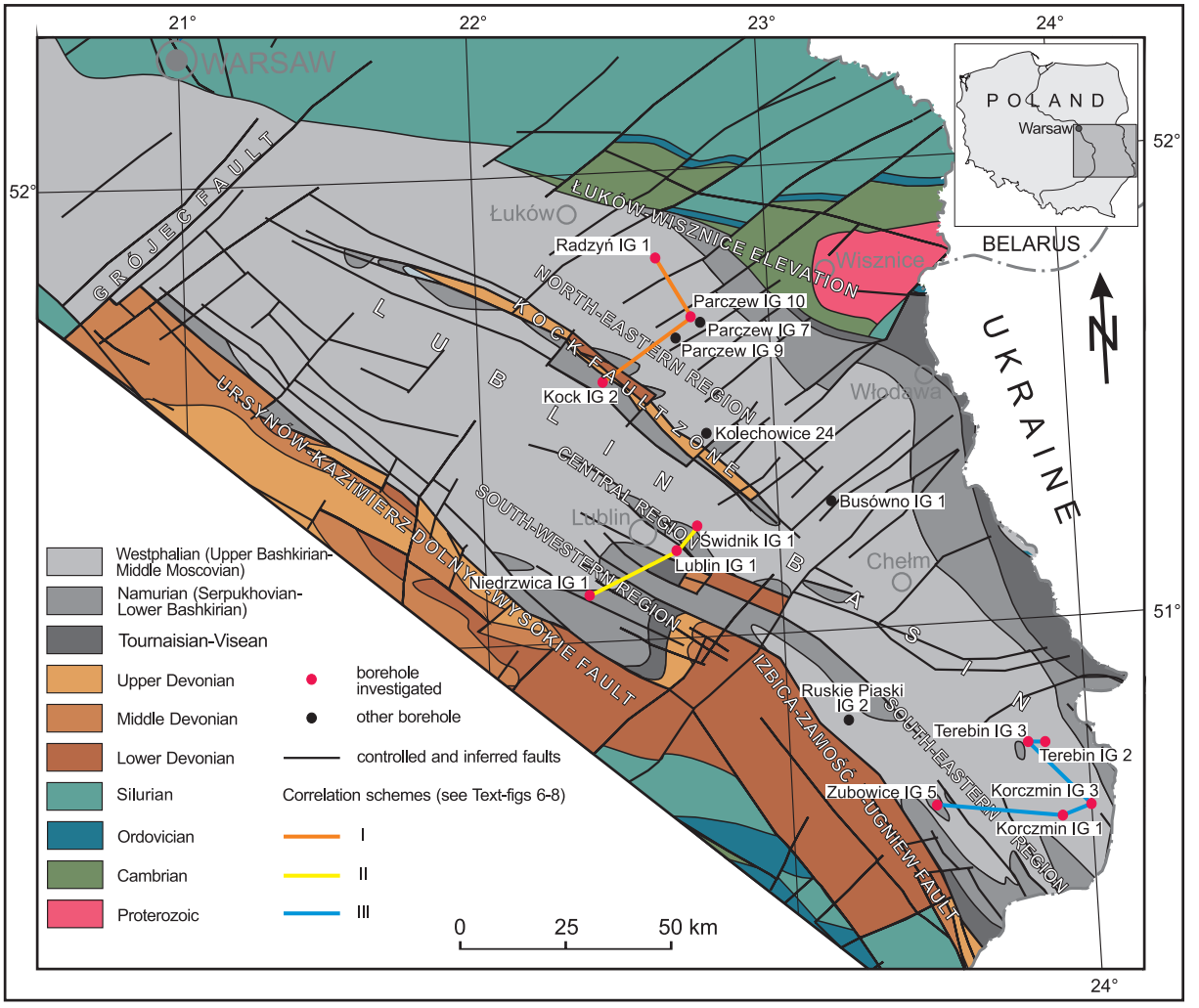

Text-fig. 1. Geological-structural map of the Lublin Basin (modified from Waksmundzka and Buła 2020), with location of the boreholes studied.

the Huczwa Formation; Text-fig. 2) in the lithostratigraphic subdivision of Porzycki and Żelichowski (1977, *fide* Porzycki 1979), has been considered variously as belonging to the Middle Visean (Żelichowski 1969, 1972; Waksmundzka 2010a) or the Upper Visean (Porzycki and Żelichowski 1977, *fide* Porzycki 1979). These rocks are palaeontologically barren. Their age was not sufficiently documented, being based on dating of the volcanic rocks (Depciuch 1974; Porzycki 1988; Grocholski and Ryka 1995) and on the latest Visean age of the upper part of the Huczwa Formation (Sołokija Member; Text-fig. 2), well-dated on the basis of fossil fauna (Musiał and Tabor 1979, 1988; Skompski and Soboń-Podgórska 1980; Soboń-Podgórska 1988; Soboń-Podgórska and Tomaś 1995; Skompski 1996) and flora (Migier 1988; Kmiecik 1988). The oldest part of the Carboniferous succession was also dated by the method of sequence stratigraphy (Kozłowska and Waksmundzka 2020) and assigned tentatively to the late Tournaisian. The putative Tournaisian age of these rocks is supported by new dating of basalts in the NE part of the Lublin Basin (Pańczyk and Nawrocki 2015), by sequence stratigraphic correlation combined with detailed petrographic research, and by correlation with the oldest part of the Carboniferous section in the Lviv-Volyn Basin, where palaeontologically well-dated Upper Tournaisian is found (Szulga 1956; Shulga *et. al*. 2007; Kostyk *et al*. 2016).

The present study focuses on the rocks ascribed to the Kłodnica Member in the context of sequence stratigraphy. The main objective is to analyse sequences

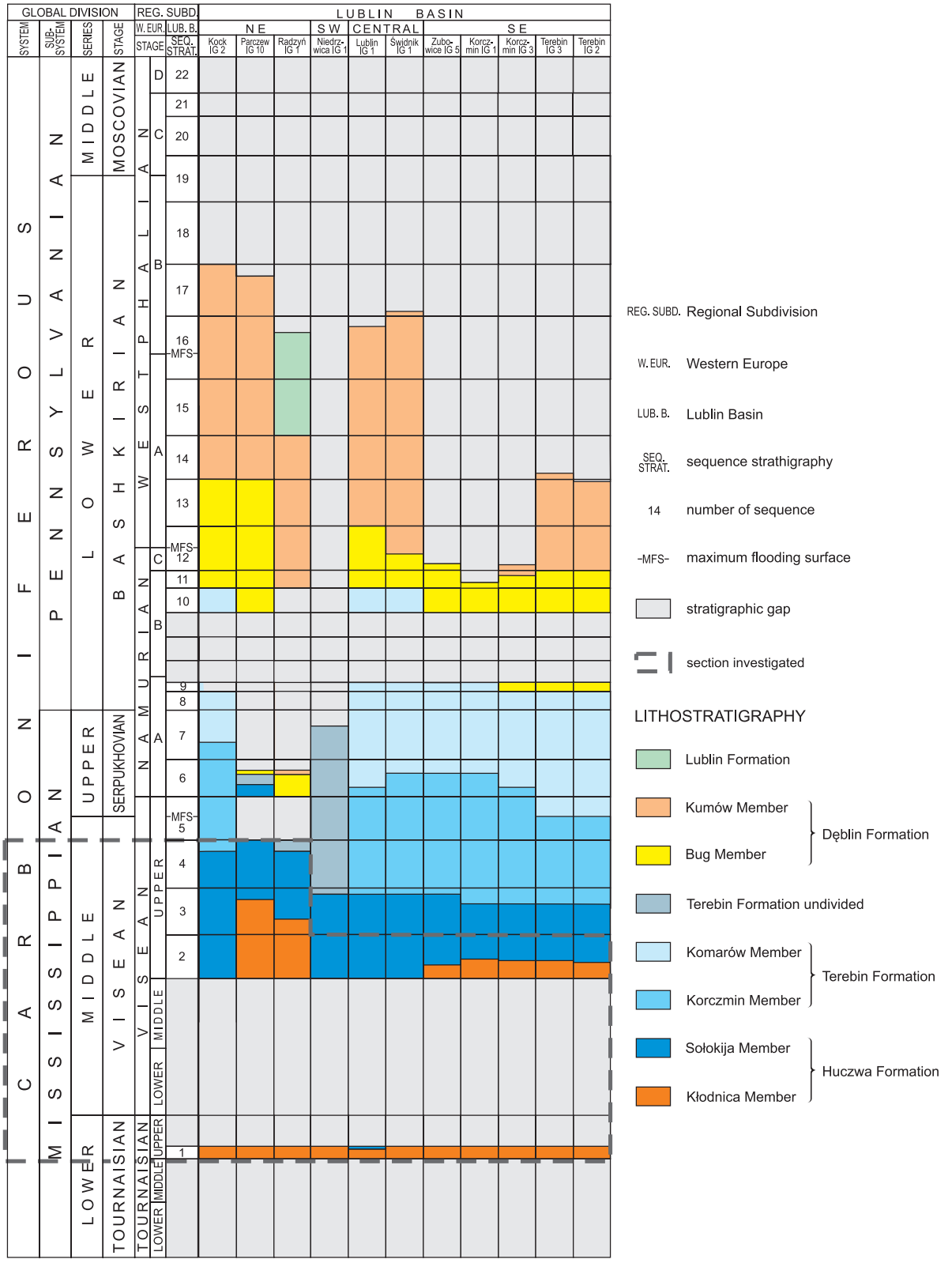

Text-fig. 2. Chronostratigraphy (after Davydov *et al*. 2012), lithostratigraphy (after Porzycki and Żelichowski 1977, *fide* Porzycki 1979) and sequence stratigraphy of the Carboniferous succession in the studied boreholes in the Lublin Basin (modified from Kozłowska and Waksmundzka 2020).

1–3 within the range of the Kłodnica Member, which covers sequence 4 in the NE area and sequences 1–2 in the remaining areas, according to the sequence stratigraphy model for the Lublin Basin given by Kozłowska and Waksmundzka (2020) and modified herein (Text-fig. 2). This is the first study providing a comprehensive description of the lithofacies, cyclicity, mineral composition, origin, age relationships and palaeogeography of the oldest, putative Tournaisian rocks in the Lublin Basin. The study aims to fill in the gap in the regional knowledge of the earliest history of the Carboniferous development in the Lublin Basin, while documenting an interesting case of the interplay of sedimentation and volcanism.

GEOLOGICAL SETTING

The present-day boundaries of the Lublin Basin, SE Poland, are defined based on the erosional extent of Carboniferous deposits and tectonic zones (Żelichowski 1969, 1972; Text-fig. 1), with a continuation towards the SE to the Lviv-Volyn Basin in Ukraine. The axis of the Lublin Basin trends NW-SE, and the basin is asymmetrical in its NE-SW cross-section. The NE side slopes gently towards the SW, which is related to the regional dip of the East European Craton (basement), whereas the western side of the basin has a steep slope along a tectonic boundary (Krzywiec *et al*. 2017). The central part of the basin hosts the Kock Fault Zone (Text-fig. 1).

Tomaszczyk and Jarosiński (2017) recognized several tectonic events that contributed to the formation of this latter fault zone. One of them was related to a change in the regional stress regime from contractional to extensional, with a relaxation that gave way to eruption of basaltic igneous rocks in the Visean. Narkiewicz (2007) suggests that the magmatic activity in the Lublin Basin was associated with a hot spot.

Krzywiec *et al*. (2017) provided interpretations of the deeply rooted, mostly reverse faults and associated basement uplifts in the eastern part of the basin. Tomaszczyk and Jarosiński (2017) indicated a dominant E-W direction of the faults in this part of the basin, contrary to the SW-NE trend previously suggested on regional maps (Żelichowski 1972; Pożaryski and Dembowski 1983; Żelichowski and Kozłowski 1983).

The Lublin Basin formed on the SW flank of the East European Craton (Mazur *et al*. 2006, 2010), with subsidence driven probably by tectonic displacements along the Teisseyre-Tornquist Lineament in a pull-apart regime (Żelichowski 1987; Narkiewicz *et al*. 1998; Krzywiec and Narkiewicz 2003; Narkiewicz 2007). The tectonic style of the basin development is attributed to less intense thin-skinned deformation (Krzywiec and Narkiewicz 2003; Krzywiec 2007; Krzywiec *et al*. 2017; Tomaszczyk and Jarosiński 2017; Kufrasa *et al.* 2019).

Carboniferous sedimentation in the Lublin Basin was preceded by erosion during the latest Devonian (Narkiewicz 2007) to Early Tournaisian and lasting until the Middle Visean in some areas. The Carboniferous succession overlies Upper Devonian rocks in the central, SW and SE parts of the basin, and lower Paleozoic and upper Proterozoic rocks in the NE part (Text-fig. 1). The thickness of the Carboniferous succession increases distinctly towards the SW and SE. The lowest thicknesses, around 100 m, are in the NE part of the basin, where the basement is elevated, whereas the greater thicknesses of several hundred to ca. 2,000 m are in the NW, SW and SE parts. The Carboniferous is covered unconformably by Permian–Mesozoic and Cenozoic deposits ranging in thickness from 200 m in the E part to about 1,000 m in the SW part of the basin.

According to the investigations by Musial and Tabor (1979, 1988) and Porzycki and Zdanowski (1995), the Carboniferous succession in the Lublin Basin is represented by deposits of Upper Visean to Westphalian D. However, Pańczyk and Nawrocki (2015) and Kozłowska and Waksmundzka (2020) subsequently suggested that Carboniferous sedimentation in the basin commenced between the Late Tournaisian and early Moscovian.

The currently used lithostratigraphic subdivision was formulated by Porzycki and Żelichowski (1977, *fide* Porzycki 1979). They distinguished five formations in the Carboniferous section, from the base upwards (Text-fig. 2): Huczwa Formation (with Kłodnica and Sołokija Members), Terebin Formation (with Korczmin and Komarów Members), Dęblin Formation (with Bug and Kumów Members), Lublin Formation and Magnuszew Formation. Except for its the lowermost part, the Carboniferous section is dominated by claystones, mudstones, siltstones, sandstones, conglomerates, limestones, marls, *Stigmaria* soils, carbonaceous claystones and coals. The lowermost part of the section, which is the main subject of this study (Text-fig. 2), consists of lava-flow basalts, tuffs, volcaniclastic conglomerates and sandstones, as well as bauxites and bauxite-like deposits. These rocks constitute the Kłodnica Member, whose thickness is relatively small and varies from 4 to ca. 36 m in the study area.

According to Musial and Tabor (1979, 1988), both the Kłodnica Member and the overlying Sołokija Member of the Huczwa Formation were of Late Visean age. However, the new dating of basalts in the basin indicates an older age for the Kłodnica Member, corresponding to the Late Tournaisian (Pańczyk and Nawrocki 2015).

The volcanic rocks of the Kłodnica Member were originally described as aphanitic diabases and tuffs (Żelichowski 1969, 1972), and as tuffolavas and diabase-melaphyre lavas (Porzycki and Zdanowski 1995). However, Grocholski and Ryka (1995) identified tephrite-potassium trachybasalts, and Pańczyk and Nawrocki (2015) examined alkaline basalts. The greatest incomplete thickness of the volcanic rocks is over 160 m in the Kolechowice 24 borehole (Porzycki 1988; Text-fig. 1).

According to Żelichowski (1969, 1972), the conglomerates of the Kłodnica Member contain clasts of quartz, siliceous rocks, flints, quartzite sandstones, dolomitic sandstones and mudstones, feldspars and pegmatites. The basal part of these deposits contains clasts of basement rocks, including Devonian calcareous sandstones and dolomitic mudstones.

The stratigraphically equivalent Series I of Cebulak (1988a) was described as composed of mainly coarse-grained deposits containing limestone clasts and frequently also with quartz grains. In some borehole profiles, the amount of carbonate clasts is lower in favour of kaolinite and quartz, claystone and sandstone clasts, occasionally also tuffs. Medium- and coarse-grained clastic rocks contain mainly clasts of quartz, claystone, mudstone and quartzite sandstone. Numerous clasts of granitoids, gneisses, crystalline schists, acidic volcanites and feldspars occur locally in the NE area of the basin. Carbonate rock clasts are rare. Kaolinite deposits, kaolinite-cemented conglomerates and/or bauxites occur in some profiles. They are occasionally underlain by laterite-capped tuff-lava rocks. In the W part of the basin, the rocks of Series I (Cebulak 1988a) contain limestone clasts and quartz. Beneath the lava-flow diabases, there are locally conglomeratic sandstones with clasts of acidic volcanic rocks. Pyroclastic sediment is also found.

Sequence stratigraphic analysis has allowed the distinguishing of 22 depositional sequences within the Carboniferous section in the Lublin Basin (Text-fig. 2), which have been tentatively correlated with the global pattern of eustatic changes, also revealing deviations related to the influence of local tectonic forcing (Waksmundzka 2008, 2010a, 2013; Kozłowska and Waksmundzka 2020).

MATERIAL AND METHODS

The study is based on the geological data and wireline logs from 11 boreholes located in the northeastern, central, southwestern and southeastern parts of the Lublin Basin (Text-fig. 1). Sedimentological study included the logging of drill cores and lithofacies analysis. Lithofacies are as defined by Reading (1978) and Walker (1992), and their coding follows Miall (1977, 1978), Rust (1978) and Zieliński (1992a, b, 1995). Fining-upward, coarsening-upward and non-gradational cyclothems are distinguished using the classification of Waksmundzka (1998, 2010a, 2012, 2013) and Kozłowska and Waksmundzka (2020).

Characterization of the investigated sections was supplemented on the basis of archive reports (mainly borehole summary reports), an unpublished MSc thesis (Hajdenrajch 2010), and published contributions (Niemczycka 1978; Cebulak 1989; Krassowska 1989; Waksmundzka 2007, 2010a, b, 2011; Cebulak *et al*. 2011).

The original thicknesses of deposits and the depths of incised valleys have been estimated based on the present-day thicknesses using the reduction ratio calculated according to the methods of Baldwin and Butler (1985). The values of the thickness reduction ratio used for claystone, mudstone, siltstone and tuff were 4.3 to 5.0, and for the conglomerate and sandstone were 1.2 to 1.4 (cf. Waksmundzka 2013).

The sections were interpreted and correlated using the sequence stratigraphic method described previously by Waksmundzka (2010a, 2012, 2013) and Kozłowska and Waksmundzka (2020). The depositional sequences, defined after Michum (1977), are bounded either by subaerial unconformities formed by fluvial erosion during a relative sea-level lowstand, or by their correlative conformities. These sequences are type 1 successions *sensu* Vail and Todd (1981). The subaerial unconformities were identified as fifth- or sixth-order erosional surfaces, representing beds of river channels, channel belts or incised valleys. Three categories of incised valley (small, medium and large) are distinguished, according to the classification by Ashley and Sheridan (1994).

The basic elements of sequences in the investigated borehole sections are parasequences defined after Van Wagoner (1985), distinguished as coarsening-upward, fining-upward and non-gradational cyclothems. They are combined into parasequence sets representing depositional systems tracts, as defined by Van Wagoner *et al.* (1988), Posamentier *et al*. (1988) and Helland-Hansen (2009). Three types of depositional systems tract are distinguished: (1) a forced-regres-

sive systems tract (FRST), (2) a transgressive systems tract (TST) and (3) a normal-regressive (NR) systems tract, which may develop during highstand (HST) or lowstand of sea level (LST). Depositional systems tract are separated by the maximum regression surface, the transgression or initial flooding surface (T) *sensu* Helland-Hansen and Gjelberg (1994) and the maximum flooding surface (MFS) as defined by Gastaldo *et al.* (1993) and Posamentier and Allen (1999). The MFS in wireline logs was identified as distinct gamma-ray maxima related to the clayey deepest-water lithofacies of shallow shelf, enriched in organic matter, or to some other relatively deep-water lithofacies, such as limestones or prodelta claystones.

To reconstruct the chronology of depositional events and volcanic processes, sequence 1 – representing the oldest Carboniferous deposits in the Lublin Basin – has been subdivided into elements of depositional architecture, labelled with the Roman numerals I–VI, VII.1 and VII.2. They form a hypothetical architectural model of sequence 1, which is a compilation of the partial sections from analysed boreholes. Sequence stratigraphy correlations were constructed across the NE (I), central and SW (II), and SE (III) parts of the basin (Text-fig. 1). The reference levels used are the top of sequence 4 in the NE part and the top of sequence 2 in the remaining parts, depending upon the extent of the investigated section.

The mineral composition and petrographic features of the various rocks of the Kłodnica Member were tied to the sequence stratigraphy. Petrographic research was conducted on 62 thin sections, examined with Nikon polarizing microscopes (OPTIPHOT2-POL and ECLIPSE LV100 POL). The classification of sandstones was based on a slightly modified scheme of Pettijohn *et al.* (1972), and that of conglomerates was based on Jaworowski (1987) and Ryka and Maliszewska (1991). The terminology applied for volcaniclastic rocks corresponds to the classifications by Le Maitre *et al.* (1989) and Winchester and Floyd (1977) for volcanic rocks. Thin sections that contained carbonates were stained with Evamy's solution to determine their types.

Catholuminescence (CL) analysis was used to study 14 rock samples. The tests were performed on an English equipment, so-called cold cathode, CITL MK5 model, equipped with EDX of Cambridge Image Technology Ltd., mounted on a Nikon polarizing microscope. A LEO 1430 scanning electron microscope, equipped with an Oxford ISIS 300 energy dispersion detector (EDS), was used. Six crumb samples were sputtered with coal and then with gold to observe the minerals. For some minerals, point qualitative X-ray analyses were performed using the VSP software. Eighteen polished, uncovered, coal-sputtered thin sections were examined. Of these, 29 analyses of chemical composition of carbonates were made on 11 samples of clastic rocks, and detailed analyses of volcanic rocks on six samples. X-ray analyses were carried out on eight rock samples using a Philips X'Pert PW 3020 X-ray diffractometer. Qualitative analysis of the overall phase composition and clay fraction composition was made. Samples powdered to the fractions below 0.063 mm were used for making compressed preparations that were air-dry tested at an angle of 1–26º2θ, after glycolysation, and heated to a temperature of 550ºC.

RESULTS

Lithofacies, their successions and cyclicity

Twenty six main types of lithofacies and their subtypes are distinguished in the core sections. Their characteristics, including the reference to bed forms, processes, sedimentary subenvironments and environments, are given in Tables 1 and 2. The most typical lithofacies are illustrated in Text-fig. 3A–L.

A characteristic feature of the Carboniferous deposits in the Lublin Basin is their sedimentary cyclicity (*sensu* Duff and Walton 1962; Miall 1996), the studying of which is an integral part of lithofacies analysis and enables reconstruction of depositional environments and architecture. It is also an important element of sequence stratigraphy. The lithofacies studied, with the exception of volcanites, form fining-upward (Text-fig. 4), coarsening-upward and non-gradational cyclothems (Text-fig. 5).

Fining-upward cyclothems

The main types of fining-upward cyclothems are distinguished based on the lithofacies succession (Waksmundzka 2012). The base of most cyclothems of type I and IIa is an erosional surface (Text-fig. 4). Type I is characterized by the presence of only a single part composed of coarse-grained, sandy and/or gravelly lithofacies (Table 1). Type II is composed of two parts: the lower coarse-grained (sandy and/or gravelly lithofacies) and the upper fine-grained (clayey/muddy/silty lithofacies) with occasional *Stigmaria* soils and carbonaceous claystone. Type II is subdivided into sub-type IIa, with its lower part composed of lithofacies deposited under mainly in upper flow regime and/or by hyper-

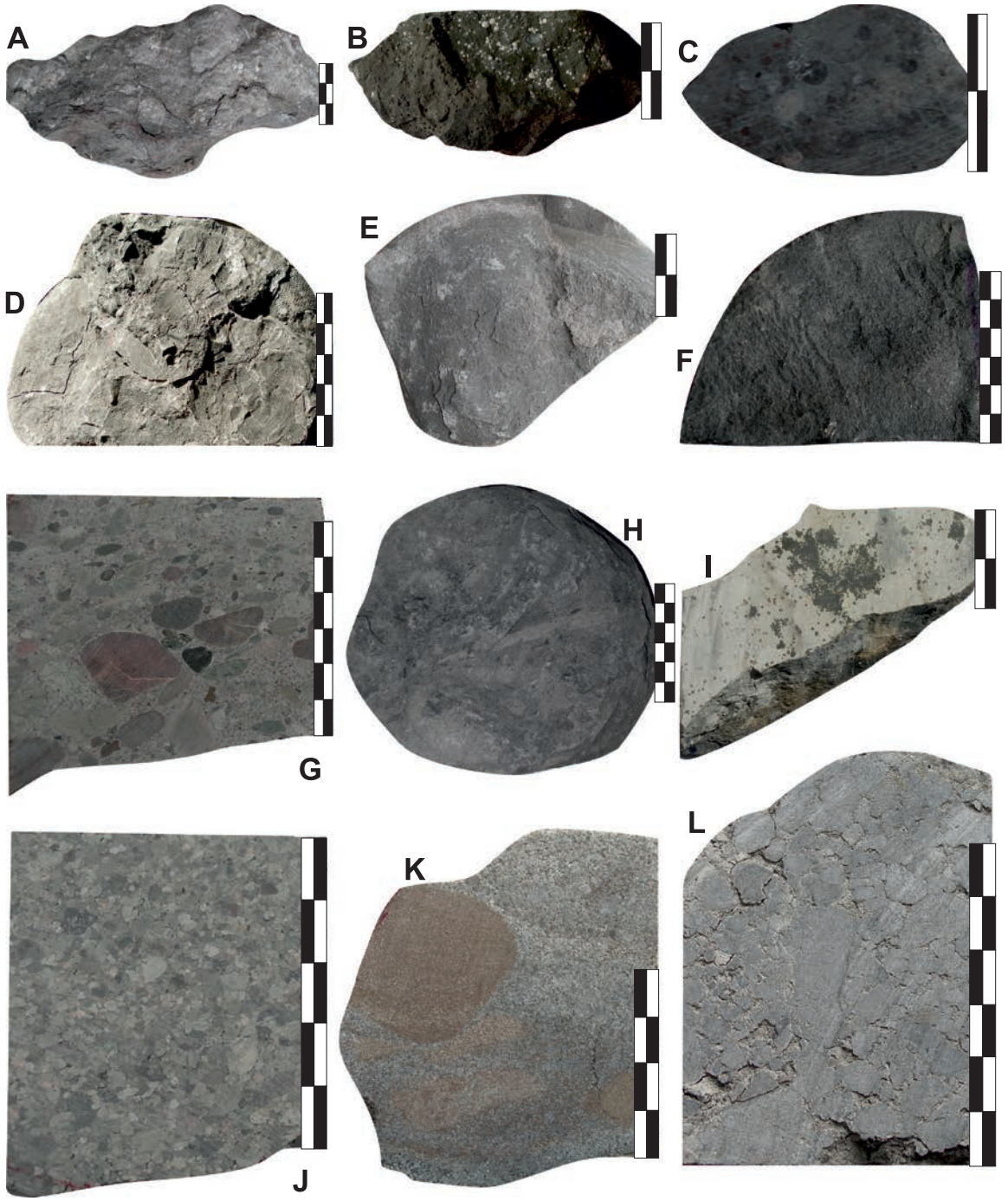

Text-fig. 3. Examples of lithofacies (scale bars = 1 cm): A – Lithofacies L: limestone with nodular structure; borehole Radzyń IG 1; HST of sequence 3; depth 923.50-923.57 m; B – Lithofacies V: basalt with amygdaloidal texture; older lava-flow; borehole Parczew IG 10; sequence 1 – element VII.2; depth 1063.4 m; C – Lithofacies V: heavily altered volcanic rock; borehole Terebin IG 3; sequence 1 – element VII.2; depth 1425.4 m; D – Lithofacies Fm1: massive claystone with bryzoans; borehole Korczmin IG 3; TST of sequence 2; depth 1349.3 m; E – Lithofacies Fm: massive claystone with siderite spherulites; borehole Radzyń IG 1; LST of sequence 4; depth 919.5 m; F – Lithofacies V: basalt; younger lava-flow; borehole Parczew IG 10; sequence 1 – element VII.2; depth 1053.2 m; G – Lithofacies GSm: massive sandy conglomerate; borehole Lublin IG 1; sequence 1 – element I; depth 2157.9 m; H – Lithofacies Fm: massive mudstone with carbonaceous plant chaff; borehole Korczmin IG 1; sequence 1 – element VI; depth 1345.2 m; I – Lithofacies T: tuff ; borehole Radzyń IG 1; sequence 1 – element VII.1; depth 941.3 m; J – Lithofacies GSm: massive sandy conglomerate; borehole Niedrzwica IG 1; sequence 1 – element V; depth 2211.9 m; K – Lithofacies GSm: massive sandy conglomerate; borehole Kock IG 2; sequence 1 – element V; depth 1597.8 m; L – Lithofacies Gm: massive conglomerate; borehole Korczmin IG 1; sequence 1 – element V; depth 1347.3 m.

Lithofacies	Structure	Colour	Flora	Process	Volcanic	Chemical weathering	Hyperconcentrated flow	Braided river	Anastomosing fluvial system	Fluvial floodplain
V Volcanic rock (Text-fig. 3B, C, F)	fine-grained, massive, porphiritic, amygdaloidal	dark green, dark grey, black, light grey-greenish-red	lack	volcanic lava-flow	■					
B Bauxite, bauxite-like rock	pelitic, clastic, laminated	light grey, cream-colored, greenish		chemical weathering of basalt and pyroclastic, standing water – deposition of aluminium hydroxide		■				
T Tuff (Text-fig. 3I)	psammite, psefite	light green-red, beige-bronze, beige, beige-red, green, green-beige		pyroclastic fall and deposition, hyperconcentrated flow	■		■			
C Carbonaceous claystone	massive	black	very common unlabeled	deposition of plant remains in peat swamp, coalification						■
R *Stigmaria* mudstone	nodular	dark grey, grey	*Stigmaria*, apendixes plant chaff	lack of flow – deposition of muddy suspension, deposition of plant remains, pedogenic						■
Fm Massive claystone and mudstone (Text-fig. 3E, H)	massive	light grey, grey, grey-green, green, beige, green-red, grey-red	plant chaff	standing water – deposition of clayey and silty suspension						■
Fh Horizontal laminated claystone and mudstone	horizontal lamination									■
FSh Horizontal laminated sandy siltstone		dark grey, grey		standing water – deposition of clayey, silty and sandy suspension						■
Fw Wavy laminated siltstone	wavy lamination			rhythmic bed load transport in current ripples and lack of flow – deposition from muddy and silty suspension						■
FSw Wavy laminated sandy siltstone										■
FSd Disturbed sandy siltstone	disturbed			bioturbations						■
Sf Flaser laminated sandstone	flaser lamination	beige, beige-dark grey, grey, grey-bronze, grey-red, grey-beige-red		rhythmic bed load transport in ripples (lower part of lower flow regime) and lack of flow – deposition from muddy and silty suspension					■	
Sr Ripple cross-stratified sandstone	ripple cross-lamination			rhythmic bed load transport in ripples (lower part of lower flow regime)				■		
Sx Large-scale cross-stratified sandstone	cross-stratification		plant chaff, carbonaceous matter	bedload transport in transverse bars or megaripples (lower or upper part of lower flow regime)			■			
Sh Horizontal stratified sandstone	horizontal stratification			deposition in upper plane bed (upper flow regime)			■	■		
Sl Low-angle cross-stratified sandstone	low-angle cross-stratification			bedload transport in transition from lower to upper flow regime				■		
Sm Massive sandstone	massive			hyperconcentrated flow			■			

Lithofacies	Structure	Colour	Flora	Process	Volcanic	Chemical weathering	Hyperconcentrated flow	Braided river	Anastomosing fluvial system	Fluvial floodplain
SGm Massive gravelly sandstone	massive	beige, beige-dark grey, grey, grey-bronze, grey-red, grey-beige-red	plant chaff, carbonaceous matter	hyperconcentrated flow			■			
SGl Low-angle cross-stratified gravelly sandstone	low-angle cross-stratification			bedload transport in transition from lower to upper flow regime			■			
SGh Horizontal stratified gravelly sandstone	horizontal stratification			deposition in upper plane bed (upper flow regime)			■			
GSm Massive sandy conglomerate (Text-fig. 3G, J, K)	massive	grey, grey-cream-colored, grey-beige, grey-bronze, grey-beige-pink, grey-green-bronze	lack	diffuse gravel sheet or longitudinal bar, transition from lower to upper flow regime				■		
Gm Massive conglomerate (Text-fig. 3L)								■		
Ge Conglomerate in erosional scours	massive with clasts	grey-yellow	large plant fragments	erosion of large scours, their filling in upper flow regime conditions				■		

Table 1. Characteristics of the lithofacies forming fining-upward cyclothems, as well as volcanic, pyroclastic and bauxite lithofacies, with an interpretation of their depositional environments.

concentrated flow, and sub-type IIb – with the lower part dominated by the lowermost-energy lithofacies Sf. The cyclothems of type IIa are the most frequent, whereas those of types IIb and I are relatively rare (Text-figs 6–8).

Cyclothems of type I, with a fining-upward trend from sandy conglomerates to sandstones or exclusively conglomerates, are signified by lithofacies succession GSm→Sm.

Their present-day thickness is 0.6–3.2 m and a decompacted calculated thickness is 0.7–4 m. The lower part of type IIa is composed of conglomerates (Text-fig. 3L), sandy conglomerates (Text-fig. 3G, J, K) and sandstones, and the upper part is dominated by clayey (Text-fig. 3E) and muddy lithofacies (Text-fig. 3H). Other lithofacies, such as *Stigmaria* soil (R) and carbonaceous claystone (C), occur in only few cases. The most typical lithofacies successions are GSm→Sh→FSh and GSm→Sm→Fm. In the second sub-type of type IIa, the typical succession is SGm→Sh→R, with no conglomerates and with the gravelly sandstones and sandstones passing directly into *Stigmaria* soil. The present-day thickness of cyclothems IIa varies from 1.6 to 23.6 m, and the decompacted calculated thickness is 4 to 69 m. For comparison, the typical lithofacies succession of the cyclothems of type IIb is Sf→Fh→R, with the present-day thickness of 7–13 m and a decompacted thickness of 22–32 m.

Coarsening-upward and non-gradational cyclothems

Based on the succession of lithofacies (Table 2) and its degree of completeness, coarsening-upward cyclothems (Waksmundzka 2010a, 2013) of types Ic and IIc and the least complete, non-gradational cyclothems of type IIIc have been recognized (Text-figs 5–8). The range of lithofacies involved defines the completeness of the cyclothem. Cyclothems Ic are composed of the following parts, from the base upwards:

– part 1: claystone lithofacies Fh1 and/or mudstone lithofacies Fh2;
– part 2: siltstone lithofacies Fn, and/or sandy siltstone lithofacies FSw;
– part 3: fine-grained sandstone lithofacies Sr and/or Sf;

Lithofacies	Structure	Colour	Flora	Fauna	Process	Shallow clayey shelf	Shallow carbonate shelf	Shallow-water delta: Prodelta	Delta front	Mouth bar	Delta plain
C Coal/carbonaceous claystone	massive	black	very common unlabeled	lack	deposition of plant remains within peat swamp, coalification						■
R *Stigmaria* claystone/mudstone	nodular	grey, dark grey, black	*Stigmaria*, apendixes, plant chaff		lack of flow – deposition of clayey or muddy suspension, deposition of plant remains, pedogenic						■
Sr Ripple cross-stratified sandstone	ripple cross-lamination	light grey	plant chaff		rhythmic bed load transport in ripples (lower part of lower flow regime)					■	
Sf Flaser laminated sandstone	flaser lamination				rhythmic bed load transport in ripples (lower part of lower flow regime) and lack of flow – deposition from muddy and silty suspension					■	■
Sh Horizontal laminated sandstone	horizontal lamination				deposition in lower plane bed from sandy suspension					■	
FSw Wavy laminated sandy siltstone	wavy lamination	dark grey, grey			rhythmic bed load transport in current and wave ripples and lack of flow – deposition from muddy and silty suspension				■		
Fn Lenticular laminated siltstone	lenticular lamination	dark grey							■		
Fh Horizontal laminated claystone and mudstone: Fh2 Horizontal laminated mudstone	horizontal lamination	dark grey, black			lack of flow – deposition from clayey and muddy suspension			■	■		
Fh Horizontal laminated claystone and mudstone: Fh1 Horizontal laminated claystone			lack	marine	lack of flow – deposition from clayey suspension	■		■			
Fm Massive claystone and mudstone: Fm3 Dark grey massive mudstone	massive		plant chaff	lack	lack of flow – deposition from clayey and muddy suspension			■			
Fm Massive claystone and mudstone: Fm2 Grey massive claystone		light grey, grey		lack/ freshwater	lack of flow – deposition from clayey suspension						■
Fm Massive claystone and mudstone: Fm1 Black massive claystone (Text-fig. 3D)		dark grey, black	lack	marine/ lack	lack of flow – deposition from clayey suspension	■		■			
M Marl		black, dark grey		marine	lack of flow – deposition from clayey suspension, deposition of limy marine fauna remains		■				
L Limestone (Text-fig. 3A)	massive, nodular	grey, filemot, greige, beige			deposition of limy marine fauna remains		■				

Table 2. Characteristics of the lithofacies forming coarsening-upward and non-gradational cyclothems, with an interpretation of their depositional environments.

– part 4: *Stigmaria* soil lithofacies R, with or without coal lithofacies C.

Two sub-types of cyclothem Ic are distinguished, with upward successions 1→2→3→4 and 1→2→3. The present-day thickness of cyclothems Ic is 7–23 m, and their decompacted thickness is 27–117 m. The main difference between these cyclothems and others of that type, described previously

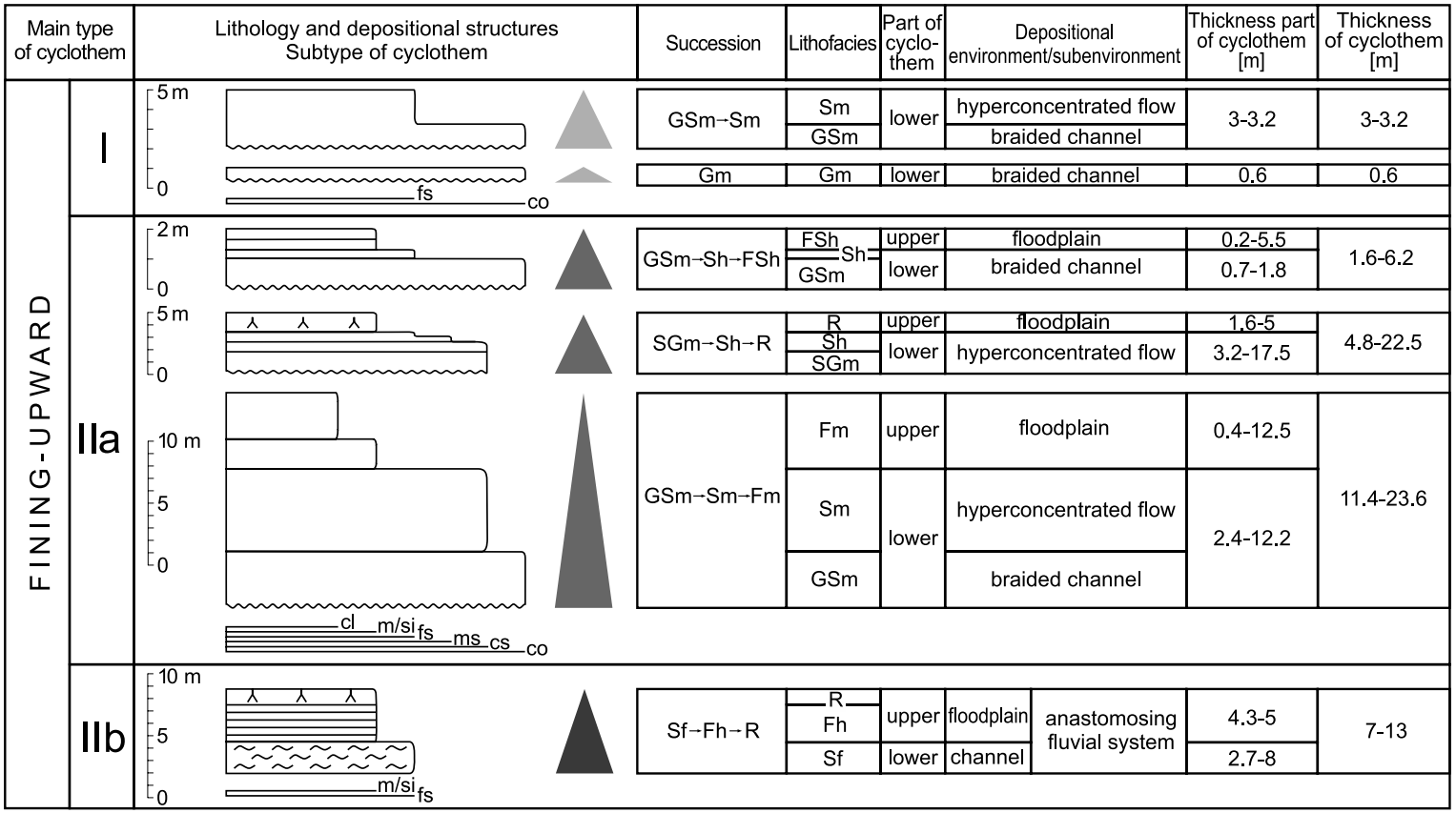

EXPLANATIONS TO TEXT-FIGS 4–5

LITHOLOGY

coal	cl	claystone
carbonaceous claystone	m/si	mudstone/siltstone
Stigmaria soil	fs	fine-grained sandstone
marl	ms	medium-grained sandstone
limestone	cs	coarse-grained sandstone
erosional surface	co	conglomerate

STRUCTURE

massive	wavy lamination
horizontal stratification	lenticular lamination
ripple-cross lamination	horizontal lamination
flaser lamination	

Text-fig. 4. Schematic examples of the fining-upward cyclothems of type I, IIa and IIb with their interpreted depositional environments.

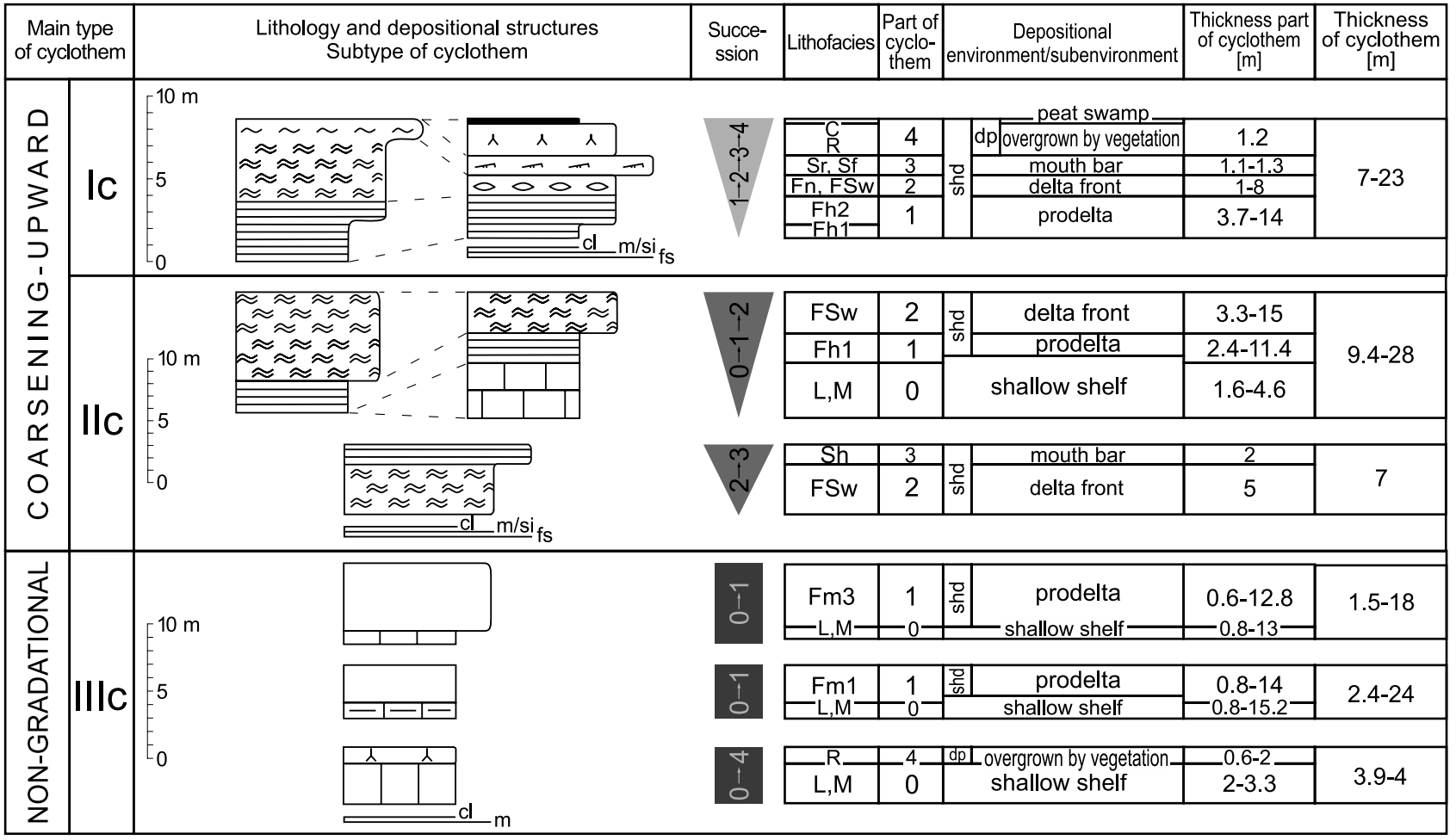

Text-fig. 5. Schematic examples of coarsening-upward cyclothems of type Ic and IIc and nongradational cyclothems of type IIIc with their interpreted depositional environments; dp – delta plain; shd – shallow-water delta.

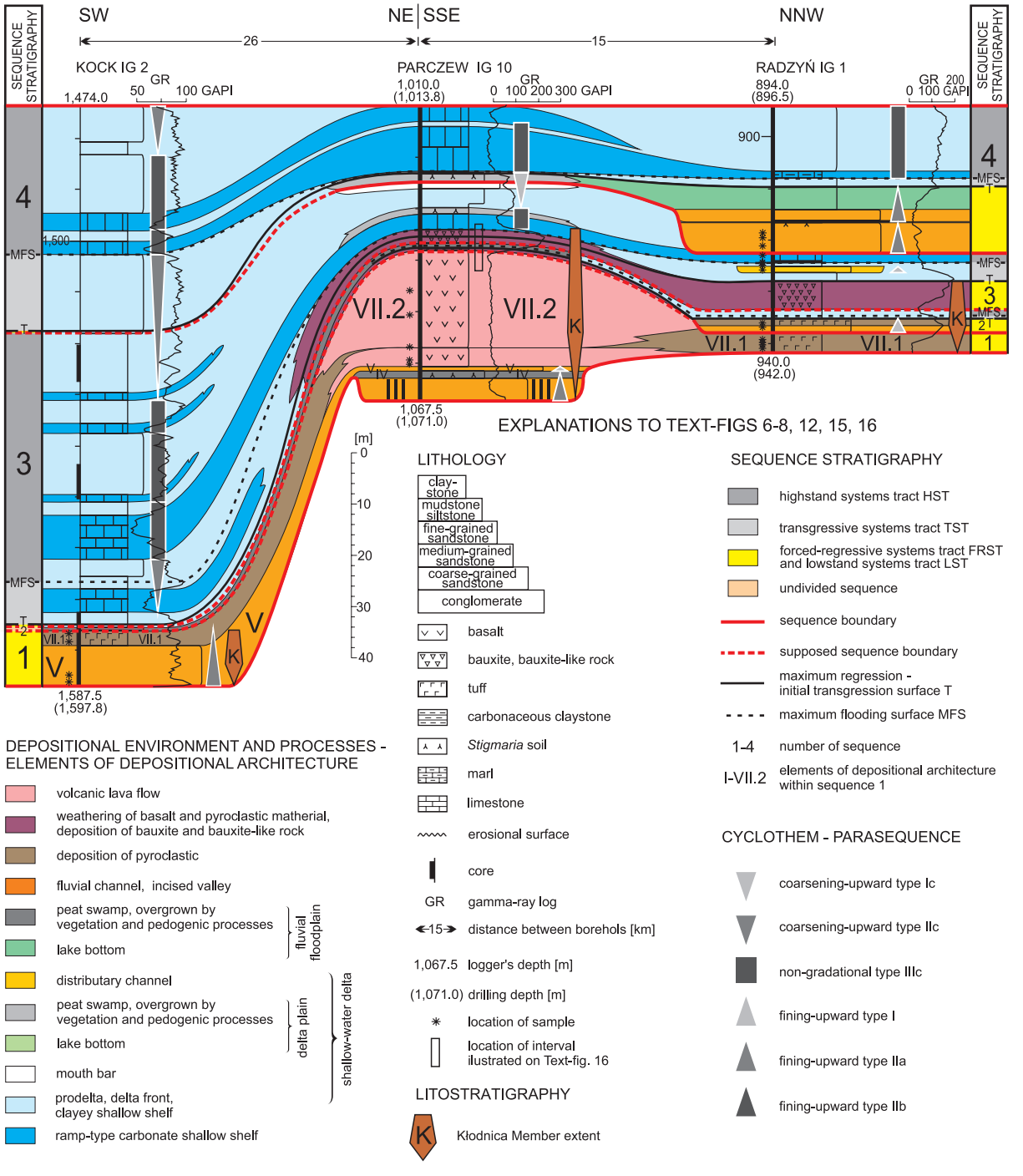

Text-fig. 6. Lithofacies correlation of the ?Tournaisian and Visean sequences 1–4 in the NE area of the Lublin Basin – scheme I; for details see online version.

by Waksmundzka (2010a, 2013), is the lack of basal shallow-shelf lithofacies L and/or M (see part 0 in Text-fig. 5).

The incomplete cyclothems of type IIc (Text-fig. 5) generally lack part 4 as well as part 3 or 1. The full spectrum of their component parts is:

– part 0: limestone lithofacies L (Text-fig. 3A);
– part 1: claystone lithofacies Fh1;

– part 2: sandy siltstone lithofacies FSw;
– part 3: fine-grained sandstone lithofacies Sh.

The three sub-types IIc are 0→1→2, 1→2 and 2→3, with the lack of part 4 distinguishing them from cyclothem varieties of this type described from other boreholes (Waksmundzka 2010a, 2013). Their present-day thickness is 7–28 m, and the decompacted thickness is 28–130 m.

The non-gradational cyclothems of type IIIc show no obvious upward grain-size trend and consist of the lower part 0 (lithofacies L and/or M) and the upper part 1 represented by lithofacies Fm1 (Text-fig. 3D), Fh1 and/or Fm3. Their present-day thickness is 1.5–24 m, and the decompacted thickness is 5–74 m. The upward succession 0→1 is most frequent in the SE part of the study area, where the available borehole sections do not show the two other sub-types of cyclothem IIIc, namely successions 0→1→4 and 1→4, described from elsewhere by Waksmundzka (2010a, 2013). However, the Parczew IG 10 and Korczmin IG 1 boreholes revealed a related succession sub-type 0→4 (Text-fig. 5).

INTERPRETATION

Depositional environments and processes

Fining-upward cyclothems

The base of the fining-upward cyclothems of types I and IIa is a surface of fluvial erosion. It is overlain by massive conglomerates Gm deposited as a diffuse gravel-lag sheet (Hein and Walker 1977), or by sandy conglomerates GSm (Table 1; Text-fig. 4) representing probably low-relief gravelly longitudinal bars that formed directly after channel incision with the highest flow power and gravel transport (Nemec and Postma 1993). These lithofacies, passing upwards into massive sandstones Sm, developed probably as a result of sediment-laden hyperconcentrated flows, whose sediments commonly show massive structure and poor sorting (cf. Nemec and Steel 1984; Svendsen *et al*. 2003). Some cyclothems of type IIa commence with gravelly sandstones SGm attributed to the same kind of process.

These types of deposits can accumulate in flash flood conditions characterized by high-energy flow and high sediment load (Batalla *et al*. 1999) during the filling of fluvial channels and incised valleys (Martinsen 1994). The dominance of massive lithofacies indicates a high sediment depositional rate (Arnott and Hand 1989). These processes are typical for valley filling during a relative sea-level rise. Hyperconcentrated flow deposits that filled incised valleys were also described by Waksmundzka (2010a, 2012) in the Bashkirian of the Lublin Basin and by Kędzior (2016) in the Lower Pennsylvanian of the Upper Silesia Coal Basin (S Poland).

When the flow energy and sediment concentration of a hyperconcentrated flow decreased, tractional bedload transport and aggradational deposition occurred in those channels, as evidenced by lithofacies Sh and SGh formed in the upper flow regime plane-bed conditions and by lithofacies SGl and Sl formed at the transition from an upper to a lower flow regime (Zieliński 2015). Similar lithofacies assemblages, interpreted as being deposited in a shallow high-energy braided river environment, were described by Tunbridge (1981) from the Devonian of Great Britain.

The occasional small decompacted thickness (<3 m) of cyclothems I and the lower part of cyclothems IIa found in boreholes to the SE is probably related to sedimentation in isolated, shallow, sand-bed braided channels. In the remaining areas of the basin, such cyclothem thicknesses indicate deposition in multistorey, gravel-bed braided channels with hyperconcentrated flows within incised valleys, usually 5–25 m deep.

The upper parts of the fining-upward cyclothems of type IIa consist mainly of the fine-grained lithofacies Fm, Fh and/or FSh, deposited from suspension in stagnant water bodies within a fluvial floodplain. *Stigmaria* mudstones R, developed by pedogenic processes in areas covered by vegetation, are rare at the top of these cyclothems. One cyclothem includes carbonaceous claystone lithofacies C, formed by coalification of plant remains deposited in a peat swamp.

The decompacted thickness of the upper parts of cyclothems IIa reaches ca. 50 m, indicating the highest aggradation of floodplain deposits in the SW area (borehole Niedrzwica IG 1) and the central area (borehole Lublin IG 1) of the Lublin Basin.

Fining-upward cyclothems of type IIb are rare. One such, found in borehole Lublin IG 1, represents probably a low-energy anastomosing fluvial system (cf. Smith 1983; Waksmundzka 2013), as indicated by a considerable thickness proportion of overbank deposits (80%) and a low proportion of channel-fill sandstone lithofacies Sf formed under a very low-energy current from muddy and silty suspension fallout.

Coarsening-upward and non-gradational cyclothems

Coarsening-upward cyclothems are common in deltaic successions (Scruton 1960; Coleman and

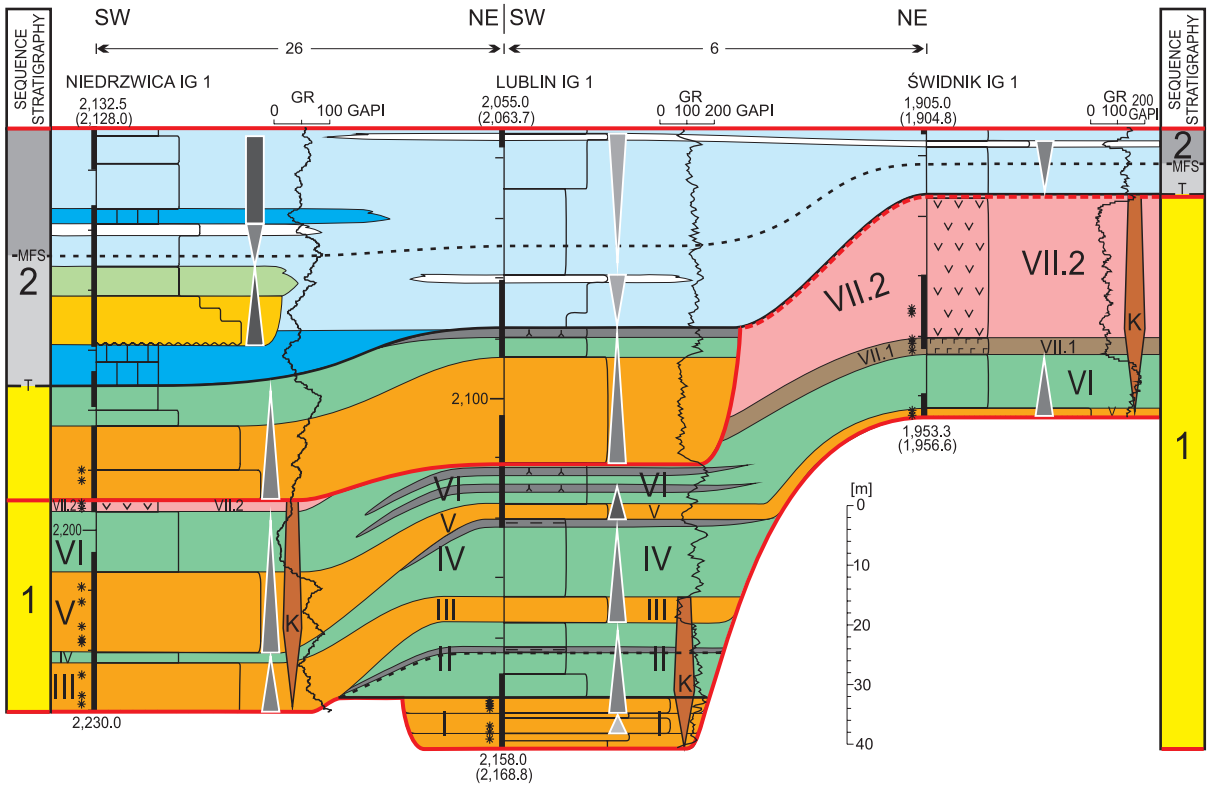

Text-fig. 7. Lithofacies correlation of the ?Tournaisian and Visean sequences 1 and 2 in the central and SW areas of the Lublin Basin – scheme II; for details see online version.

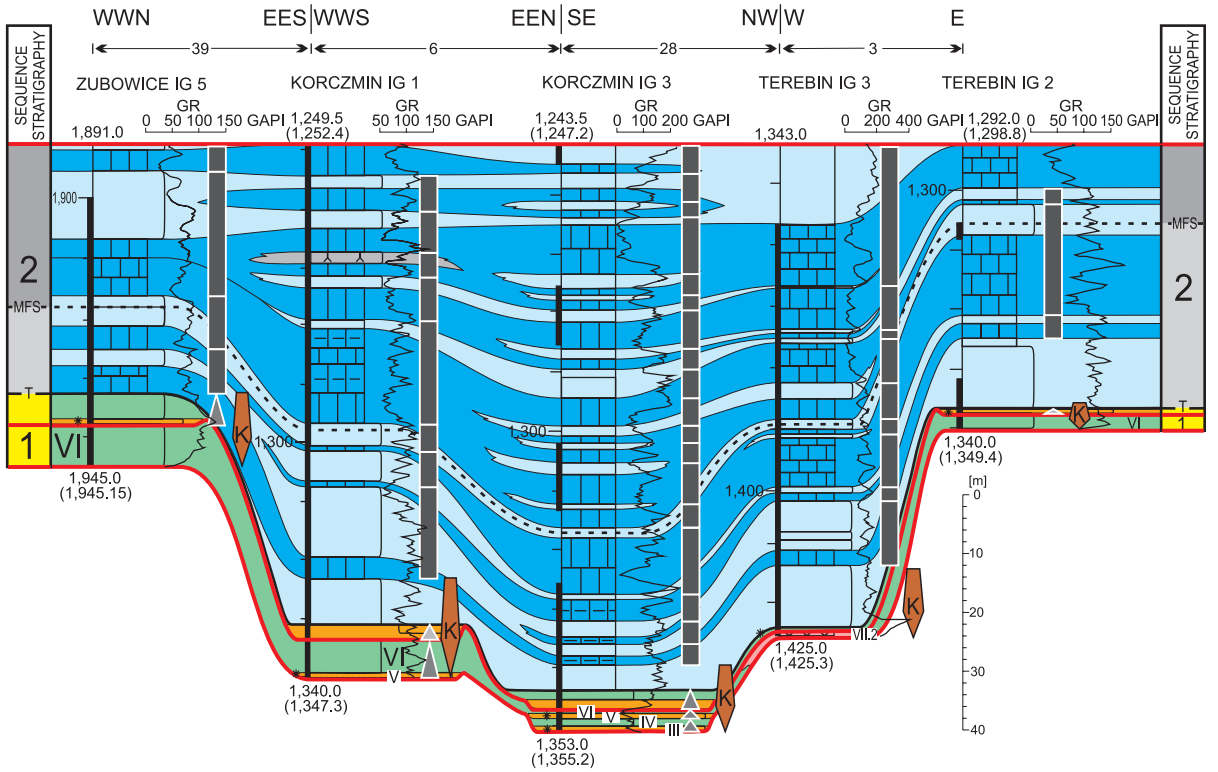

Text-fig. 8. Lithofacies correlation of the ?Tournaisian and Visean sequences 1 and 2 in the SE area of the Lublin Basin – scheme III; for details see online version.

Wright 1975; Elliot 1974, 1975, 1976a, b, 1978) and such features have been similarly recognised in the Carboniferous sections in the Lublin Basin (Waksmundzka 2010a, 2013; Kozłowska and Waksmundzka 2020). These cyclothems in the studied borehole sections comprise parts 0 to 4 and are categorized as complete cyclothems Ic and incomplete cyclothems IIc (Text-fig. 5), with lithofacies characteristic of muddy deltaic sub-environments and shallow carbonate or clayey shelf environments (Table 2). Part 0 at the base of some of the cyclothems of type IIc consists of lithofacies L (limestone) and/or M (marl), developed in a shallow-marine, ramp-type carbonate shelf environment with three zones of different wave energy (cf. model by Flügel 2004). Detailed characteristics of this environment have been discussed by Skompski (1988, 1995) and Waksmundzka (1998, 2010a, 2013).

The carbonate shelf was separated from land by a vast zone of deltaic lobes. Above part 0 of a cyclothem, there is part 1 composed of claystone lithofacies Fm1/Fh1 and mudstone lithofacies Fh2. The claystones and mudstones, characterized by black colour and high radioactivity (interpreted from well logs), developed most likely on a shallow clayey shelf at a delta fringe. More frequent are dark grey claystones and mudstones containing benthic fauna (bivalves, brachiopods, corals and bryozoans), deposited in prodelta sub-environment.

The overlying part 2 consists usually of siltstones Fn and sandy siltstones FSw accumulated in an active submarine zone of delta lobe aggradation – on a delta slope (Wright and Coleman 1974; Wright 1977), which is a heterolithic zone of mud, silt and very fine-grained sand, commonly with considerable amounts of plant detritus (Pulham 1989; Hampson *et al*. 1999). The higher-lying part 3 consists of fine-grained sandstone lithofacies Sr, Sf and Sh, deposited in a mouth bar zone close to the mouths of delta-plain distributary channels (cf. Coleman and Wright 1975; Elliot 1978; Turner and Whateley 1983; Miall 1986; Einesele 1992).

The fine-grained deltaic system – with its prodelta, delta slope and mouth bar sub-environments – prograded onto a shallow marine shelf. The topmost part 4 of some cyclothems (Text-fig. 5) represents the subaerial delta plain, where sedimentation occurred in swamps (carbonaceous claystones lithofacies C) and vegetated areas (*Stigmaria* palaeosoil lithofacies R). The deposition of fine-grained sandstone lithofacies Sf in delta-plain distributary channels resulted in the formation of the associated fining-upward cyclothems of type IIb described in the previous section.

The coarsening-upward cyclothems would then represent a fluvial-dominated shallow-water delta with a delta plain of type D according to the Postma (1990) classification. In the classification of shelf deltas by Porębski and Steel (2003), the Carboniferous deltaic system in the Lublin Basin would represent inner-shelf deltas.

The borehole profiles show also non-gradational cyclothems of type IIIc (Text-fig. 5), which are genetically related to the coarsening-upward cyclothems and known as well from other sections in the Lublin Basin (Waksmundzka 2010a, 2013; Kozłowska and Waksmundzka 2020). Their most frequent sub-type is a bipartite succession 0→1, formed in the migrating environments of shallow carbonate or clayey shelf and prodelta. Another sub-type is bipartite succession 0→4, indicating an abrupt emergence of shelf ramp and the formation of a vegetated subaerial plain.

PETROGRAPHIC CHARACTERISTICS

The sedimentary succession with its cyclothems is generally non-volcanic, but includes volcaniclastic and volcanic rocks. The volcaniclastic rocks are products of the mechanical disintegration of volcanic material in various environments (cf. Fisher and Schmincke 1984; Łydka 1996). This group of rocks contains pyroclastic material mixed in various proportions with non-volcanic sediment (Ryka and Maliszewska 1991). In this paper, pyroclastic rocks are called tuffs and the mixed pyroclastic-epiclastic rocks are called volcaniclastic conglomerates and sandstones. The petrographic characteristics of the most typical microlithofacies are described in the present chapter (Text-figs 9A–F, 10A, B, 11A–F).

Conglomerates

The massive sandy conglomerates of lithofacies GSm (Table 1) are fine- and very fine-grained polymictic paraconglomerates and are volcaniclastic (Text-fig. 9A, B), except in borehole Kock IG 2 (Text-fig. 9C). These rocks show a psephitic texture and a non-oriented fabric, only locally slightly aligned, with a linear arrangement of clay flakes and flatter pebbles. The content of the gravel fraction varies from about 30% to approximately 85%, with the dominant grain size of 2–10 mm and maximum size of >21–60 mm. Clasts consist of rounded, subrounded and angular rock fragments as well as grains of quartz and feldspar.

Lithoclasts are mainly fragments of volcanic rocks and sandstones, accompanied by fragments of clay-

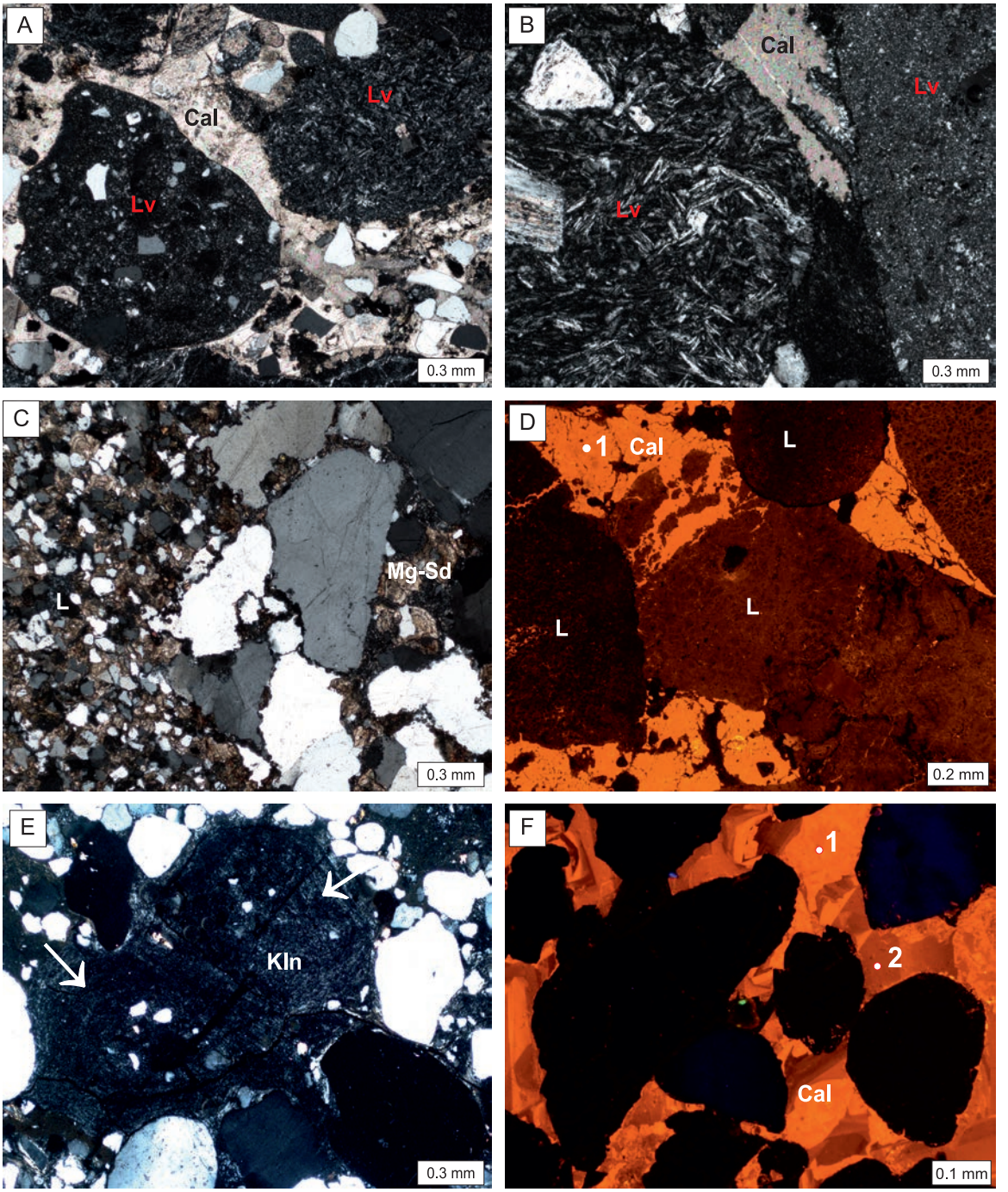

Text-fig. 9. Photomicrographs of conglomerates and sandstones taken in a polarizing microscope (PL) and cathodoluminescence (CL). A – Calcite cement (Cal) in fine-grained volcaniclastic polymictic paraconglomerate; volcanic rock fragments (Lv) are rhyolite to the left and andesite? to the right; borehole Lublin IG 1, sequence 1, element I, depth 2157.9 m; PL, crossed nicols. B – Fragment of fine-grained volcaniclastic polymictic paraconglomerate and calcite cement (Cal); volcanic rock fragments (Lv) are basalt to the left and rhyolite to the right; borehole Niedrzwica IG 1, sequence 1, element V, depth 2211.9 m; PL, crossed nicols. C – Crystals of sideroplesite (Mg-Sd) in fine-grained polymictic paraconglomerate; to the left, fragment of siderite-cemented sandstone (L); borehole Kock IG 2, sequence 1, element V, depth 1597.8 m; PL, crossed nicols. D – Orange luminescence of calcite (Cal) cement in fine-grained oligomictic ortoconglomerate (rudstone); carbonate rock fragments (L); 1 – chemical analysis point (Table 3); borehole Korczmin IG 1, sequence 1, element V, depth 1347.3 m; CL image. E – Perlite clast (arrowed) in coarse-grained volcaniclastic quartz/sublithic wacke with perlite acidic volcanic glass altered to kaolinite (Kln); borehole Terebin IG 2, LST of sequence 2, depth 1346.8 m; PL, crossed nicols. F – Calcite cement (Cal) in coarse-grained conglomeratic quartz arenite; 1, 2 numbers – chemical analysis points (Table 3); borehole Radzyń IG 1, LST of sequence 4, depth 919.4 m; CL image.

Borehole	Sequence stratigraphy and lithofacies	Depth [m]	Rock name	Point of analysis	Mg wt.%	Ca wt.%	Mn wt.%	Fe wt.%	$MgCO_3$ mol%	$CaCO_3$ mol%	$MnCO_3$ mol%	$FeCO_3$ mol%	Carbonate type
NE region													
Kock IG 2	1/V GSm (Text-fig. 3K)	1597.8 (Text-fig. 9C)	fine-grained polymictic paraconglomerate	1	1.19	3.88	1.45	38.37	4.3	10.1	3.1	82.5	sideroplesite spherulite
				2	1.92	4.74	0.28	38.20	6.8	12.0	0.6	80.6	sideroplesite
				3	1.93	4.89	0.39	38.02	6.9	12.4	0.8	79.9	sideroplesite rhombohedra
Radzyń IG 1	4 SGh	919.4 (Text-fig. 9F)	coarse-grained, conglomerate quartz arenite	1	0.00	40.65	0.38	0.17	0.0	98.9	0.8	0.3	Mn/Fe-calcite
				2	0.00	39.63	0.37	0.59	0.0	98.0	0.8	1.2	Fe/Mn-calcite
	2 T	936.2	coarse ash tuff	1	0.20	39.64	0.50	0.71	0.7	96.8	1.0	1.5	Fe/Mn-calcite
				2	1.08	0.70	1.87	43.07	3.8	1.8	4.0	90.4	sideroplesite
SW and central regions													
Lublin IG 1	1/I GSm	2157.9 (Text-figs 3G, 9A)	fine-grained volcaniclastic polymictic paraconglomerate	1	0.06	39.10	0.12	1.05	0.2	97.4	0.2	2.2	Fe/Mn-calcite
				2	0.17	38.05	1.67	0.44	0.6	95.0	3.5	0.9	Mn/Fe-calcite
		2162.1	fine-grained volcaniclastic polymictic paraconglomerate	1	0.33	36.72	2.14	1.14	1.2	91.9	4.5	2.4	Mn/Fe-calcite vein
				2	0.08	37.32	1.75	1.16	0.3	93.7	3.6	2.4	Mn/Fe-calcite vein
Niedrzwica IG 1	2 GSm	2191.6	very fine-grained volcaniclastic polymictic paraconglomerate	1	0.01	0.40	0.64	46.97	0.0	1.0	1.3	97.7	siderite
				2	2.46	1.50	2.22	39.97	8.6	3.8	4.6	83.0	sideroplesite
				3	4.27	0.35	2.75	37.79	14.9	0.9	5.8	78.4	sideroplesite
	1/V GSm (Text-fig. 3J)	2211.9 (Text-fig. 9B)	fine-grained volcaniclastic polymictic paraconglomerate	1	0.08	38.76	1.46	0.27	0.3	96.1	3.0	0.6	Mn/Fe-calcite
				2	0.10	38.73	1.17	0.34	0.4	96.5	2.4	0.7	Mn/Fe-calcite
SE region													
Korczmin IG 1	1/V Gm (Text-fig. 3L)	1347.3 (Text-fig. 9D)	fine-grained oligomictic ortoconglomerate (rudstone)	1	0.67	38.89	0.53	0.00	2.3	96.6	1.1	0.0	Mn-calcite
Korczmin IG 3	1/V GSm	1353.9	very fine-grained volcaniclastic polymictic paraconglomerate	1	0.25	37.12	2.48	0.65	0.9	92.6	5.2	1.3	Mn/Fe-calcite
				2	0.62	3.45	35.97	7.04	2.2	8.5	74.8	14.5	rhodochrosite
				3	0.00	37.94	1.25	0.73	0.0	95.4	3.1	1.5	Mn/Fe-calcite
				4	0.55	3.68	34.51	6.97	1.9	9.4	73.9	14.8	rhodochrosite
	1/III GSm	1355.1	very fine-grained volcaniclastic polymictic paraconglomerate	1	0.07	36.82	3.07	0.67	0.2	92.0	6.4	1.4	Mn-calcite
				2	0.07	37.89	0.55	1.99	0.2	96.5	1.2	2.1	Fe/Mn-calcite
Zubowice IG 5	2 Sm	1937.3	fine-grained sublithic/subarkosic arenite	1	0.45	37.39	0.75	1.64	1.6	93.4	1.6	3.4	Fe/Mn-calcite
				2	0.23	38.84	0.84	0.70	0.8	95.0	1.8	1.4	Mn/Fe-calcite
				3	6.31	22.66	1.13	8.57	22.4	57.2	2.4	18.0	ankerite
				4	0.19	38.69	0.49	0.62	0.7	97.0	1.0	1.3	Fe/Mn-calcite

Table 3. Chemical composition of carbonates based on microprobe analyses.

stones, mudstones, siderite rocks and metamorphic quartz schists. Subordinate are fragments of plutonic rocks (granitoids and granodiorites). Clasts of volcanic rocks include rhyolites, dacites, andesites, basalts and volcanic glass (Text-fig. 9A, B). Sandstone clasts have a very fine- to medium-grained texture and represent quartz arenites with a clay-silica matrix and with quartz, siderite (Text-fig. 9C), calcite, pyrite and kaolinite cements. The conglomerates contain also quartz grains, poly- and monocrystalline and

Borehole	Sequence stratigraphy and lithofacies	Depth [m]	Rock name	Quartz	Na-Ca Feldspar	Carbonates			Anatase	Hematite	Clay minerals		
						Siderite	Magnesite	Dolomite			Kaolinite	Illite/Smektite	Chlorite
Kock IG 2	1/VII.1 T	1594.7	pumice tuff			+			+		+		
Lublin IG 1	1/I Sm	2165.6	medium-grained volcaniclastic lithic arenite/wacke	+	+					traces	+	+ 80% Illite	+
Niedrzwica IG 1	2 GSm	2190.0 (Text-fig. 10A)	very fine-grained volcaniclastic polymictic paraconglomerate	+	+	traces						+ >90% Illite	+
	1/V GSm	2218.4	very fine-grained volcaniclastic polymictic paraconglomerate	+	+		traces	traces				+ 85% Illite	+
Terebin IG 2	2 Sh	1346.8 (Text-fig. 9E)	coarse-grained volcaniclastic quartz/sublithic wacke	+		+					+		+
Terebin IG 3	1/VII.2 V (Text-fig. 3C)	1425.4 (Text-figs 10B, 11F)	heavily altered acid volcanic rock							+	+		

Table 4. XRD analyses; + presence.

of volcanic origin (angular, with corrosion bays), as well as rare feldspar grains. Lithoclasts and feldspars commonly show the effects of silicification, chloritization, argillitization, carbonatization and hematitization processes.

The space between gravel clasts is filled with a fine- to coarse-grained sandy matrix, which has a quartz arenite or quartz wacke composition in sequence 1 in the NE and SE areas, and lithic or arkosic arenite composition in the central and SW areas. In sequence 2, the sand matrix is a subarkosic wacke. Sand grains consist mainly of mono- and polycrystalline volcanic quartz, feldspar and fragments of predominantly acidic volcanites, quartzites, sandstones, micropertites and granitoids. There are also single mica flakes and heavy minerals, with abundant anatase(?) and zircon. The sand matrix is cemented with quartz, authigenic clay minerals (kaolinite, chlorites, illite), carbonates (Fe/Mn-calcite, Mn/Fe-calcite, siderite, sideroplesite, rodochrosite) (Text-fig. 9A–C; Table 3), pyrite, iron oxide, detrital clay mineral and silica. X-ray analyses of the clay mineral composition show the presence of mixed-layer illite/smectite minerals (with an illite content >85%) and chlorite (Table 4).

The massive conglomerates of lithofacies Gm, found only in borehole Korczmin IG 1 in the SE area of the basin, are fine-grained, calcareous oligomictic orthoconglomerates (Text-fig. 9D) with a different composition. They contain ca. 50–80% of gravel fraction and have mainly a clast-supported texture. The gravel clasts are subrounded fragments of carbonate rocks with a dominant size of 6 mm and maximum size of 25 mm. Clasts represent crystalline limestones with micrite-, microsparite- and sparite-sized crystals, including pyrite. The sand-silt matrix contains clay, clasts of carbonate rocks, infrequent quartz grains and scattered clasts of non-carbonate rocks (volcanic glass, quartzite), as well as a kaolinite, pyrite and Mn-calcite cement.

Sandstones

The sandy lithofacies include massive sandstones (Sm) and horizontal stratified sandstones (Sh) or gravelly sandstones (SGh). In terms of composition, the most common are volcaniclastic sandstones (Text-fig. 9E) represented by fine- to coarse-grained, locally pebbly, lithic/sublithic arenites recognized in the NE, central and SW parts of the basin. Less common are sublithic/subarkose arenites or sublithic wackes found in the SE part. Detrital material is rounded, subrounded to angular, most often poorly sorted, locally well sorted.

The main framework grain components are quartz, feldspars, lithoclasts, as well as single micas (biotite, muscovite) and accessory minerals (zircon, anatase). Detrital quartz grains are mostly monocrystalline, rarely polycrystalline. Volcanic quartz with corrosion bays is recognizable. Feldspars are mainly albite and microcline, mostly altered, showing the effects of argillitization, chloritization, carbonatiza-

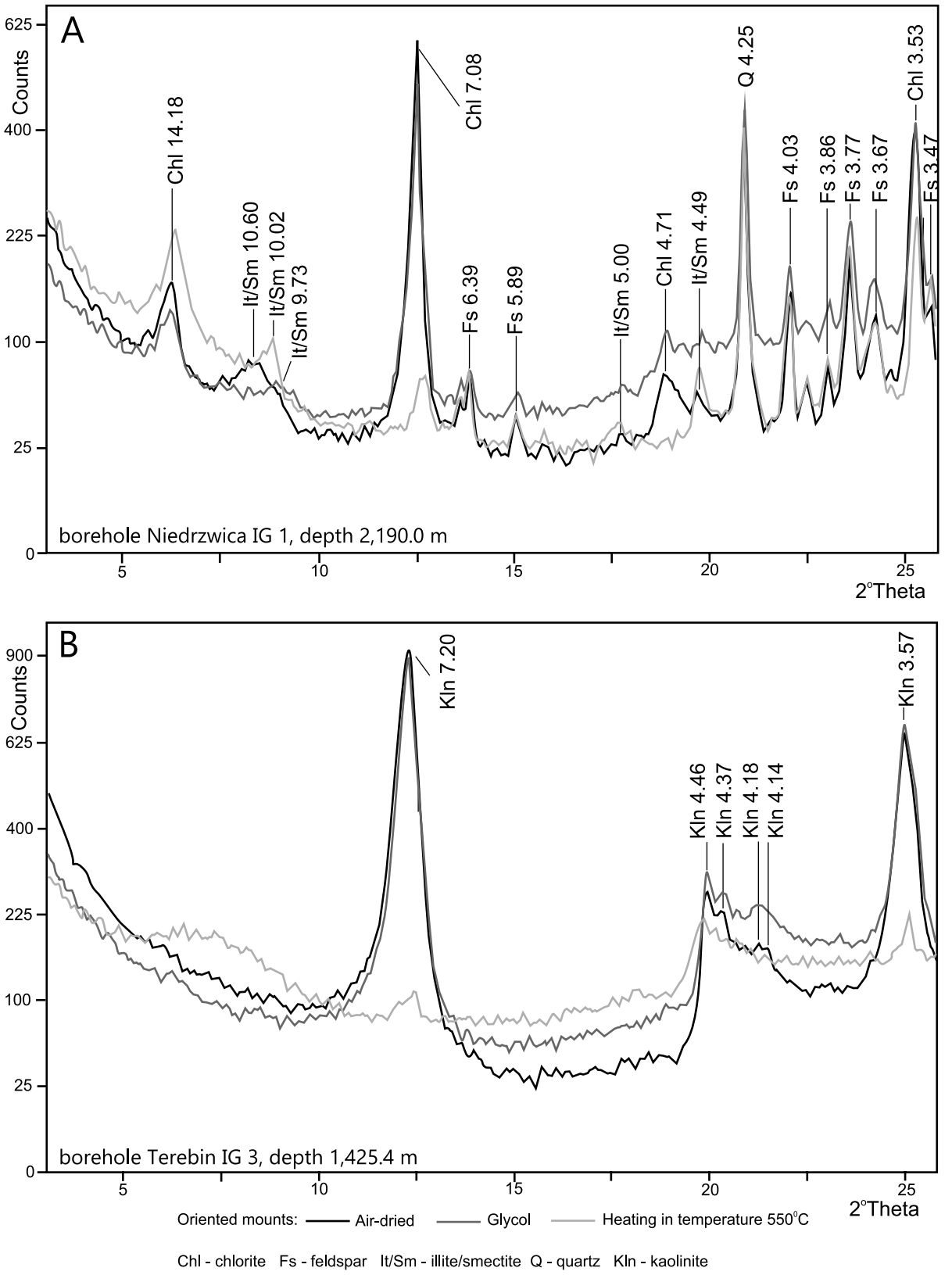

Text-fig. 10. XRD diagrams of the clay fraction. A – Very fine-grained volcaniclastic polymictic paraconglomerate; borehole Niedrzwica IG 1, depth 2190.0 m. B – Heavily altered acidic volcanic rock; borehole Terebin IG 3, depth 1425.4 m.

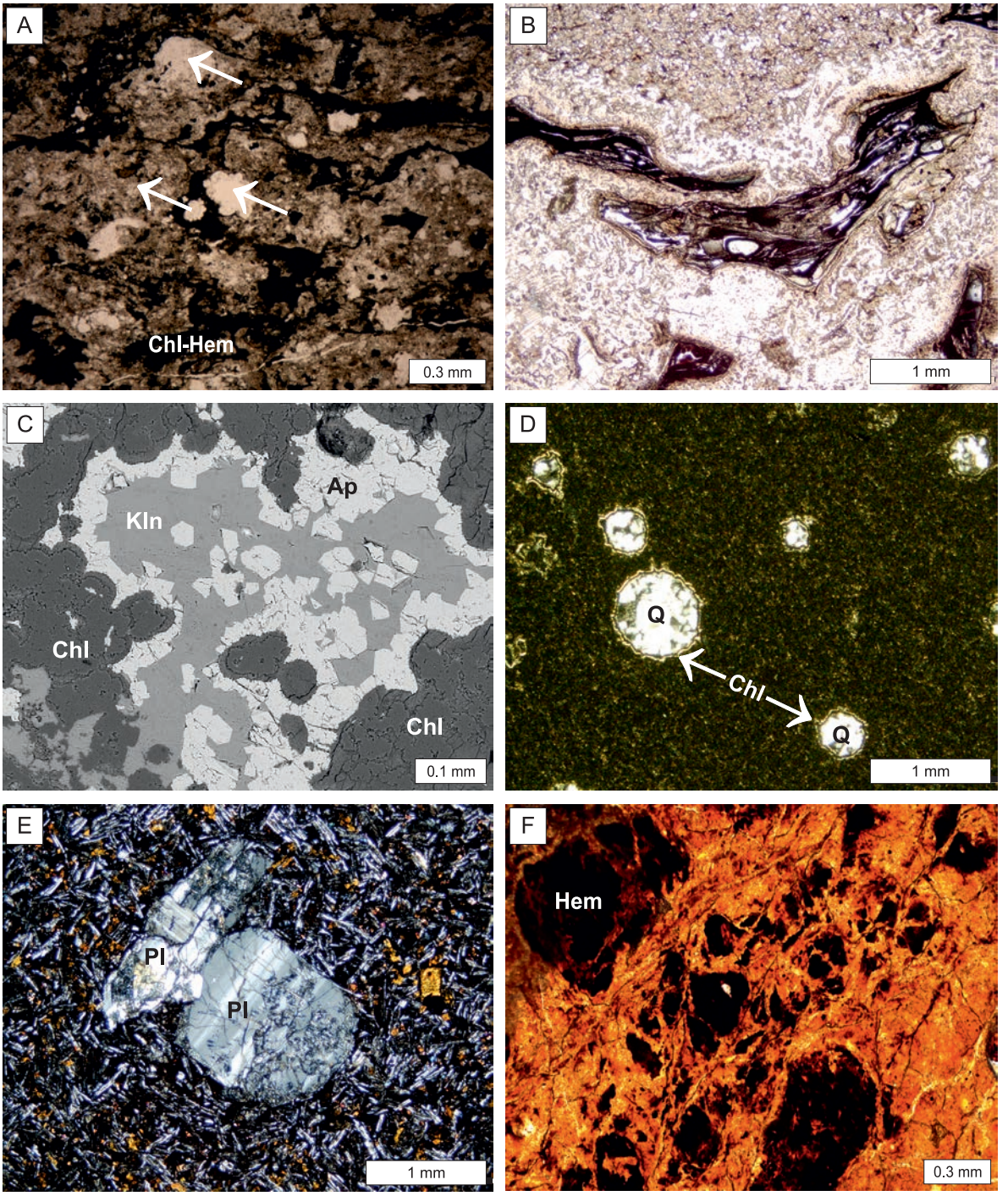

Text-fig. 11. Photomicrographs of tuffs and volcanic rocks taken in a polarizing microscope (PL), cathodoluminescence (CL) and back-scatter electron image (BSE). A – Coarse ash tuff; fragments of volcanic glass altered to kaolinite (arrows) in chlorite-hematite matrix (Chl-Hem); borehole Radzyń IG 1, sequence 1, element VII.1, depth 941.3 m; PL, without analyser. B – Strongly altered tuff with slightly welded pumice; borehole Świdnik IG 1, sequence 1, element VII.1, depth 1941.5 m; PL, without analyser. C – Tuff – chloritization (Chl) and kaolinitization (Kln) of volcanic glass (volcanic ash) with apatite crystals (Ap); borehole Świdnik IG 1, sequence 1, element VII.1, depth 1941.5 m; BSE. D – Older lava-flow alkaline basalt; amygdaloidal texture, vesicles filled with chlorite (Chl) and quartz (Q); borehole Parczew IG 10, sequence 1, element VII.2, depth 1064.5 m; PL, crossed polars. E – Younger lava-flow alkaline basalt with plagioclase (Pl) phenocrysts; borehole Parczew IG 10, sequence 1, element VII.2, depth 1053.2 m; PL, crossed polars. F – Perlitic texture of heavily altered acidic volcanic rock with hematite (Hem) concentrations in kaolinite-hematite matrix; borehole Terebin IG 3, sequence 1, element VII.2, depth 1425.4 m; PL, without analyser.

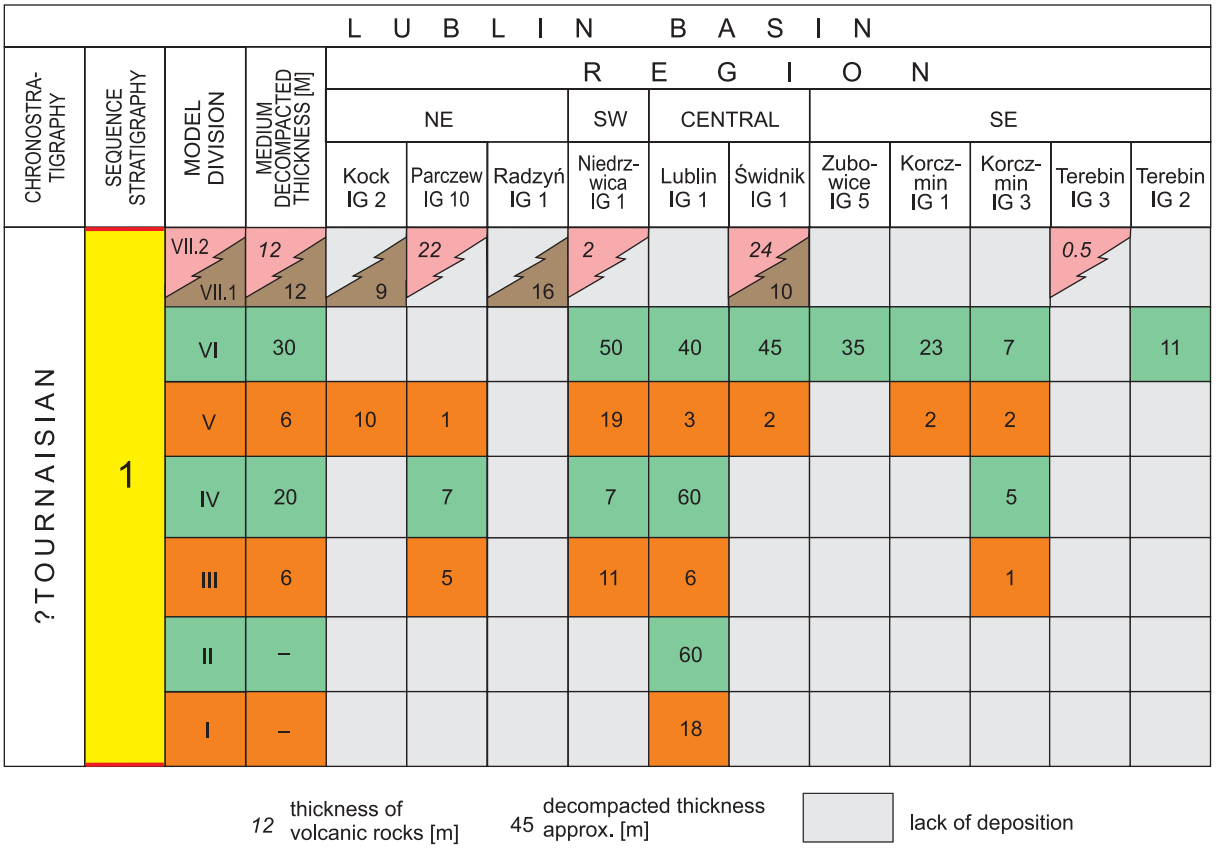

Text-fig. 12. Hypothetical model for the development and division of sequence 1 into elements of depositional architecture; for explanation, see Text-fig. 6.

tion and hematitization. Lithoclasts represent metamorphic rocks (quartz schists) and very fine-grained sandstones (quartz arenites and wackes), volcanic rocks (mainly rhyolites, andesites and basalts, rarely dacites) and volcanic glass shards. They commonly show the effects of argillitization, silicification, calcitization, kaolinitization (Text-fig. 9E), chloritization, sideritization and hematitization.

The grains are cemented with a clay-silica matrix or a clay-ferruginous matrix, as well as authigenic clay minerals (kaolinite, chlorite, illite, illite/smectite with an 80% illite content) (Table 4). Some of the authigenic clay minerals were the result of alteration of volcanic glass. The rocks contain also carbonate cements, mainly siderite (finely crystalline and spherulitic), calcite, Mn/Fe-calcite, Fe/Mn-calcite and ankerite (Table 3), as well as quartz cement (overgrowths on quartz grains), pyrite and hematite.

Another sandstone variety consists of fine-grained quartz arenites and medium- to coarse-grained gravelly quartz arenites (Text-fig. 9F), found only in borehole Radzyń IG 1 in the NE area of the basin. They are mainly massive, with subrounded and well sorted grains. The main framework grain component is quartz, mainly monocrystalline. Micas occur in trace amounts, altered to kaolinite. An accessory is zircon. The main cement components are clay-silica matrix, vermiform kaolinite, quartz (overgrowths on quartz grains) and pyrite. Present also are carbonates: siderite and Mn/Fe-calcite (Text-fig. 9F; Table 3).

Tuffs

Tuffs have been found in three boreholes. In borehole Radzyń IG 1 to the NE (Text-fig. 6), a strongly altered coarse ash tuff (Text-fig. 3I) consists mainly of fragments of pumice-type porous volcanic glass changed into kaolinite (Text-fig. 11A) and with chlorites replaced by hematite. The fragments of volcanic glass are flattened, with an oriented "flow" fabric. In addition, there are clasts of rhyolite-type volcanic

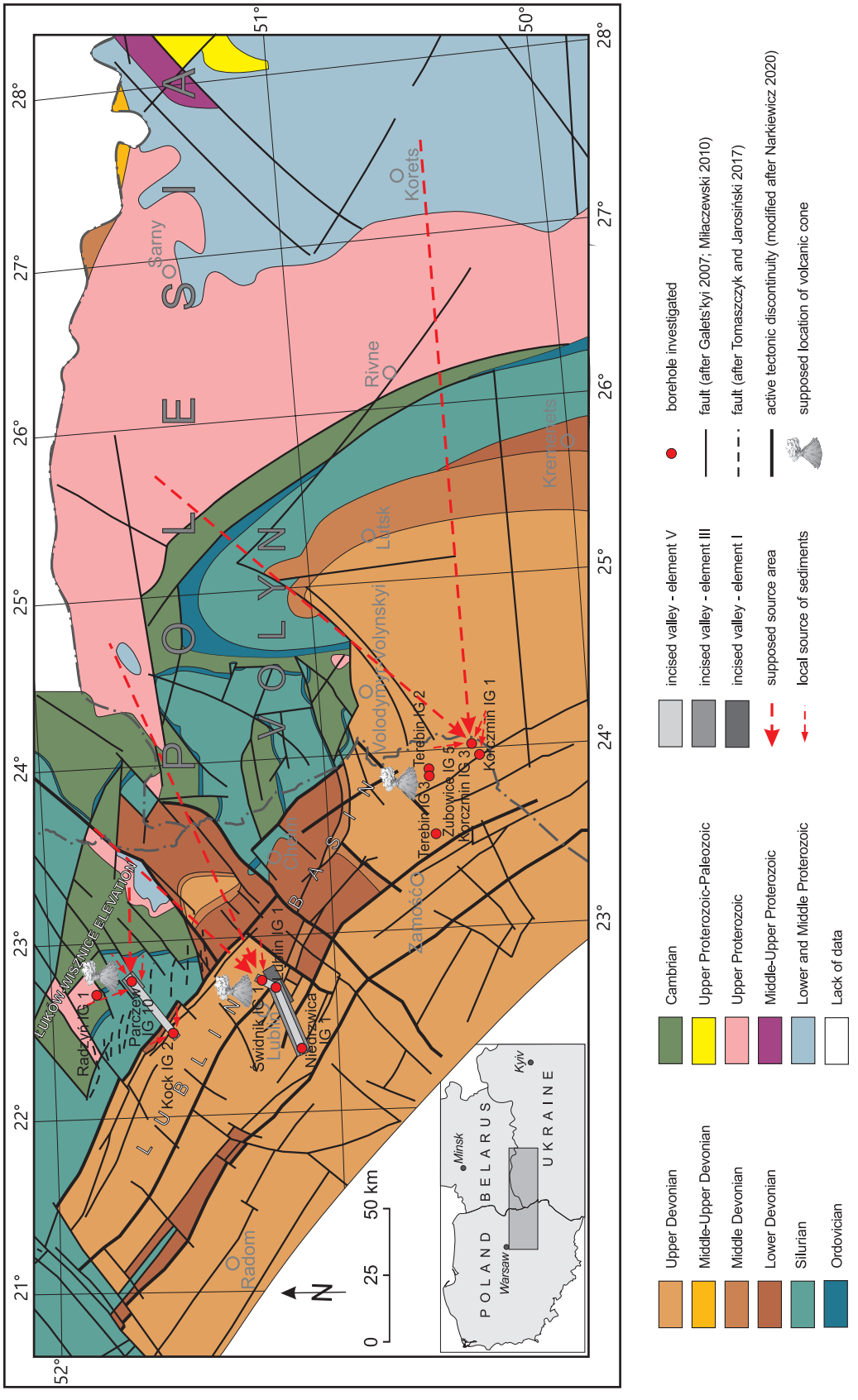

Text-fig. 13. Palaeogeological map of the Carboniferous basal erosional unconformity surface in the Lublin Basin (modified from Miłaczewski 2010) and the adjacent Volynian Polesia (modified from Galets'kyi 2007), with the inferred location of incised valleys, volcanic cones and source areas during the deposition of sequence 1.

rock and monocrystalline quartz grains, some of volcanic origin, with corrosion bays. The rock contains variable amounts of heavy mineral grains (anatase?) and light-colour mica flakes. The rock is cemented with kaolinite, chlorite and hematite. Carbonate minerals are siderite and Fe/Mn-calcite (Table 4), rhombohedral in shape. Pyrite is also common.

In borehole Kock IG 2 (Text-fig. 6), a pumice tuff deposit consists of the black flattened lenses of volcanic glass and pumice (fiamme?). It shows a directional "flow" fabric marked by the orientation of detrital anatase, clay particles and siderite. Clay is kaolinite (Table 4), probably a product of volcanic glass alteration. Sideritization is common, with siderite in the form of radial spherulites.

In borehole Świdnik IG 1 in the central part of the basin (Text-fig. 7), a highly altered tuff was found under basalts. Intensely chloritized glass shards were observed in the transformed fine-grained (metasomatized) mass, which was most likely a volcanic ash in origin. Detrital material has not been found. In the upper part of the section, fragments of pumice or scoria were observed, with signs of slight compression (Text-fig. 11B). The rock groundmass is represented most likely by recrystallized and altered ash, strongly kaolinitized and chloritized (Text-fig. 11C).

Volcanic rocks

Volcanic rocks from the group of alkaline basalts were found in several boreholes in the Lublin Basin. In borehole Parczew IG 10 in the NE area (Text-fig. 6), these volcanic rocks represent two consecutive lava-flows. The first, older lava-flow basalt is characterized by a fine-grained, amygdaloidal texture (Text-fig. 3B). The vesicules are filled with either chlorite alone or with chlorite, kaolinite and quartz (Text-fig. 11C, D). Phenocrysts were not observed. The strongly altered groundmass (mostly chloritized) contains plagioclase laths and accessory minerals, such as rutile and apatite (Text-fig. 11D). The younger lava-flow basalt is characterized by porphyritic texture (Text-fig. 3F), with plagioclase phenocrysts (labradorite-andesine) up to 20 mm in length (Text-fig. 11E). The groundmass consists of altered glass, plagioclase laths and olivine and pyroxene crystals. Analcime is the most probable mineral between the laths of plagioclase. The rock is evidently altered.

In borehole Świdnik IG 1 in the central area (Text-fig. 7), the volcanic rock is the younger lava-flow basalt, characterized by porphyritic texture. The groundmass consists of plagioclase laths, clinopyroxene, altered olivine and analcime. Common accessory minerals are apatite and ilmenite.

In borehole Niedrzwica IG 1 to the SW (Text-fig. 7), the volcanic rock has a porphyritic, intersertal to intergranular texture and represents the younger lava-flow basalt. Plagioclase phenocrysts are rare. The altered groundmass contains laths of plagioclase of andesine composition, probably post-olivine pseudomorphoses, hydrothermal quartz and K-feldspar. The main accessory minerals are apatite and ilmenite. The rock is cut by microveins filled with hydrothermal minerals, such as calcite, chlorite and quartz.

In borehole Terebin IG 3 to the SE (Text-fig. 8), a heavily altered volcanic rock was found (Text-figs 3C, 11F). The rock is characterized by a perlitic texture, which is typical of devitrified acidic volcanic glass (cf. Siemaszko 1978; Ryka and Maliszewska 1991; Rottella and Simandl 2004; Al-Mashaikie and Al-Hawbanie 2010). The kaolinite-hematite groundmass (Text-fig. 10D; Table 4), which could be formed as a result of alteration and replacement of volcanic glass, hosts numerous oval hematite accumulations (pseudomorphoses after grain replacement) and single angular psammitic and aleuritic quartz grains. This occurrence of presumed acidic extrusive volcanic rocks, presently highly altered, is herein reported for the first time from the Lublin Basin. Previously, only alkaline effusive rocks, diabase-melaphyres (Porzycki and Zdanowski 1995), tephrite-potassium trachybasalts (Grocholski and Ryka 1995) and alkaline basalts (Pańczyk and Nawrocki 2015) were reported from the basin, although signs of acidic volcanism were detected by Popek (1986) from volcaniclastic rocks.

SEQUENCE STRATIGRAPHY

The ensuing sequence-stratigraphic interpretation of the studied sedimentary-volcanic succession, with a distinction of four sequences (labelled 1–4), refers to Text-figs 6–8 and 12. The basic concepts of sequence stratigraphy are after Van Wagoner *et al.* (1988) and Catuneanu (2006). However, we follow Helland-Hansen (2009) in distinguishing three basic types of systems tract as the building blocks of sequences: a forced-regressive systems tract (FRST) formed during a relative sea-level fall; a transgressive systems tract (TST) formed during a relative sea-level rise; and a normal-regressive (NR) systems tract, which may form during highstand (HST) or lowstand of sea level (LST).

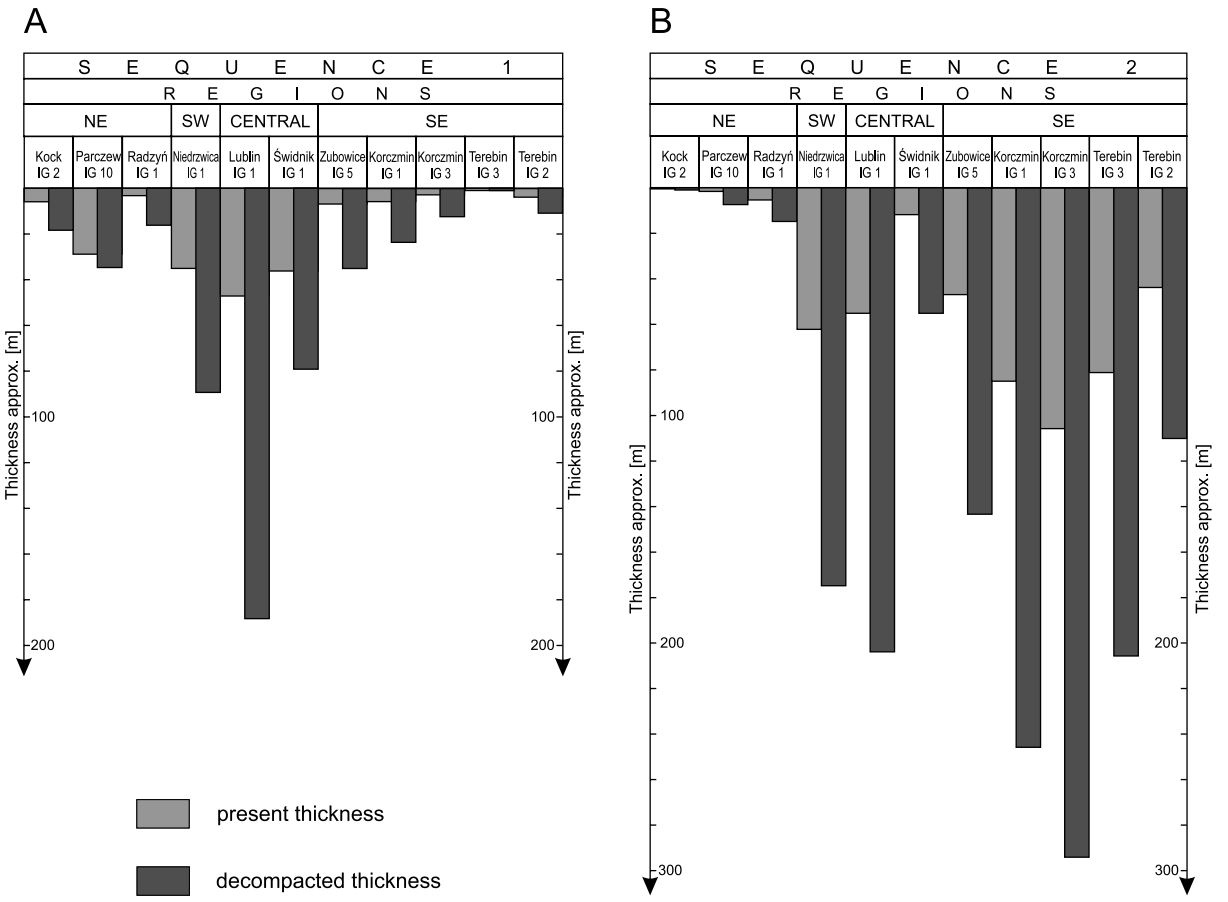

Text-fig. 14. Comparison of the present-day and decompacted thicknesses in the investigated boreholes sections. A – Sequences 1; B – Sequence 2; the thickness reduction ratio used for claystones, mudstones, siltstones and tuffs is 4.3–5.0 and for conglomerates and sandstones is 1.2–1.4 (after Waksmundzka 2013, supplemented).

Sequence 1

The present-day (compacted) thickness of sequence 1 is greatest in the central and SW areas of the basin, with a maximum exceeding 47 m in borehole Lublin IG 1 (Text-fig. 14A). Much smaller are its thicknesses in the NE and SE areas, where they generally do not exceed a few metres. The interpreted palaeogeography during the development of sequence 1 is illustrated in Text-fig. 13.

FRST and LST

The onset of Carboniferous sedimentation was preceded by the strongest denudation in the Lublin Basin (Bojkowski and Dembowski 1988). Erosional processes were most pronounced in its NE part, in the area of the Łuków-Wisznice Elevation, which was subject to a strong differential tectonic uplift (Cebulak 1988b). The Devonian deposits there were completely eroded and the lower Paleozoic to Proterozoic rocks became exposed. Various Devonian units were concurrently exposed in the rest of the basin area (Galets'kyi 2007; Miłaczewski 2010).

As the relative sea level (RSL) was falling, the river channels cut down and formed incised valleys in the pre-Carboniferous bedrock (FRST). The base of sequence 1 is an erosional base of the Carboniferous deposits, with an incised valley recognized in the central part of the basin (borehole Lublin IG 1). As the RSL subsequently stabilized, the medial incised valley, ca. 18 m deep, was filled with deposits of gravel-bed braided channels and hyperconcentrated flows, forming the division element I (early LST) of the sequence (Text-fig. 12). This is considered to be the oldest architectural element of the Carboniferous succession in

the Lublin Basin. It comprises the fining-upwards cyclothems of type I and the lower part of cyclothem IIa. The valley-fill massive sandy conglomerates GSm and sandstones Sm are polymictic and poorly sorted, indicating a relatively short distance from the source area. The grain sizes of lithofacies GSm are comparable; usually up to several millimetres in size, with a minor amount of larger flat elongate clasts up to 30 × 60 mm in size. These are grains of volcanic quartz, quartz arenite, rhyolite, andesite, basalt, granodiorite, granitoid, feldspar and volcanic glass.

After the infilling of the valley, a low-energy limnic plain developed, probably as a terminal floodplain of the fluvial drainage system (stratigraphic element II), considered to represent the late LST. These deposits form the upper part of the fining-upward cyclothem IIa. The lacustrine claystones and mudstones have a decompacted thickness of ca. 60 m, which indicates considerable basin-floor subsidence. As the subsidence declined and a deficit of accommodation space occurred, the fluvial system extended its route over the floodplain, forming a small incised valley (element III) with a depth of ca. 5–6 m in the area of boreholes Lublin IG 1 and Parczew IG 10 (Text-fig. 15A). The valley depth increases towards the SW to ca. 11 m in borehole Niedrzwica IG 1. In the central area of the basin, the valley incised into the floodplain deposits of element II. Isolated fluvial channels developed in the SE area, as evidenced by a palaeochannel ca. 1 m thick in borehole Korczmin IG 3. The erosion probably reached the Upper Devonian in the least subsided areas to the SW and SE, and perhaps even Silurian in the NE area.

The deposits of element III form the lower part of fining-upward cyclothem IIa. The incised valley in the Lublin-Niedrzwica area was filled with deposits of gravel-bed braided channels and hyperconcentrated flows. In the Niedrzwica IG 1 borehole, the valley-fill consists of massive sandstones Sm, lithic or volcaniclastic sublithic arenites. They contain quartz, feldspars, volcanic glass and volcanic rocks, including rhyolite and andesite. There are also gravel-sized clasts of effusive rocks, as well as intraformational flat claystone clasts, 3 × 10 mm in size. The grains are subrounded or angular and poorly sorted, which supports the notion of a short transport and local sediment derivation. In borehole Parczew IG 10, the valley-fill consists of massive gravelly sandstones SGm with clasts of claystone, quartzite and feldspar (Żelichowski *et al*. 2011). The isolated shallow palaeochannel in borehole Korczmin IG 3 shows the massive, volcaniclastic sandy polymictic paraconglomerates GSm with quartz arenite clasts.

As subsidence resumed, a low-energy terminal floodplain environment returned to the study area, represented by stratigraphic element IV (Text-fig. 15A). The greatest thickness of its deposits, ca. 60 m, is in borehole Lublin IG 1, where the rate of accommodation space creation was apparently highest. In the other areas, the thickness in boreholes is smaller, ca. 5–7 m.

The deposition of element V was preceded by another phase of fluvial erosion, probably due to the decline of subsidence and temporal deficit of accommodation space. This erosional episode was most pronounced in the SW part of the basin (borehole Niedrzwica IG 1), where a medium valley, ca. 19 m deep, was incised into the deposits of element IV. In the area of borehole Świdnik IG 1, the erosion reached Devonian bedrock. The valley probably had its knickpoint migrating towards the central area of the basin, where the depth of incision is smallest, increasing towards the SW. The valley-fill consists of massive sandy conglomerates GSm, representing gravel-bed braided channels and hyperconcentrated flows. The clast components include detrital and volcanic quartz, rhyolite, trachyte, andesite, basalt, volcanic glass, claystone, mudstone, sandstone, indeterminate acidic effusive rock and feldspar. Gravel clasts are subrounded, angular or rounded, poorly sorted, 2 to 16 mm in size.

In the NE area (borehole Kock IG 2), a small coeval valley, ca. 10 m deep, was incised into the Devonian bedrock (Text-fig. 15A). The valley probably had its knickpoint migrating towards the area of borehole Parczew IG 10, where a shallow, gravel-bed braided channel developed. The valley-fill deposits are massive, sandy polymictic paraconglomerates GSm composed mainly of lithoclasts, such as quartz arenites and siderite sandstones. Volcanic glass is present. Sorting is poor. Fine pebble gravel is accompanied by large, elongate flat pebbles, 7–21 × 16–48 mm in size, the largest clasts encountered in the conglomerate facies. The isolated palaeochannel in borehole Parczew IG 10 has a depth of ca. 1 m and contains large pebbles, several centimetres in size, of sandstones similar to those in element I (Żelichowski *et al*. 2011).

Shallow braided channels developed also in the SE area of the basin, incised either in the Devonian bedrock (borehole Korczmin IG 1) or in the deposits of element IV (borehole Korczmin IG 3). They are filled with massive, oligomictic calcareous orthoconglomerates of lithofacies Gm composed of subrounded carbonate lithoclasts ranging in size from a few to 10×15 mm.

A low-energy terminal floodplain was subsequently re-established and its deposits formed the

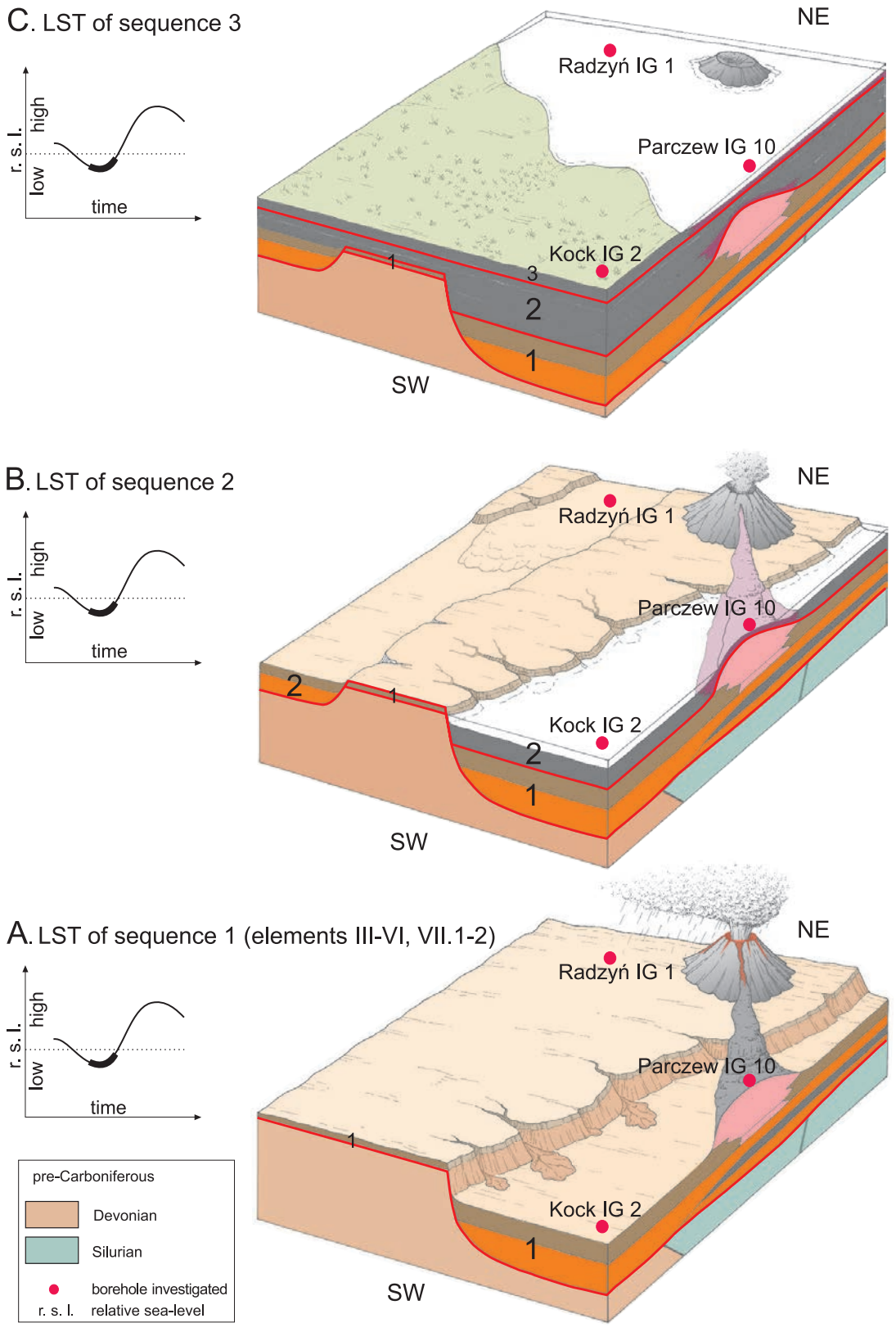

Text-fig. 15. Variation in the depositional environments and processes of the LST of sequences 1–3 in the NE area of the Lublin Basin. A – LST of sequence 1 (elements III–VI and VII.1–2); B – LST of sequence 2; C – LST of sequence 3; for further explanation, see Text-fig. 6.

stratigraphic element VI. Their decompacted thickness is in the range of ca. 40–50 m, indicating increased subsidence and greater growth of accommodation space.

The development of the LST of sequence 1, with architectural elements I–VI, is then considered to have evolved under a slowly rising base level, but being strongly modulated by an unsteady and differential, spatially non-uniform basin-floor tectonic subsidence. Localized magmatic uplift, prior to the impending phase of volcanism (see below the younger volcanic elements VII.1 and VII.2 of the LST), probably contributed to the variable subsidence regime. Under the unsteady and non-uniform forcing, the alluvial system could not sustain a constant style of sediment accumulation and, instead, showed non-equilibrium responses, as recorded by the architectural elements (sedimentary palaeoenvironments) and their changes (cyclothems) in the LST succession.

The overlying tuff element VII.1, found in the boreholes Radzyń IG 1, Kock IG 2 (Text-fig. 15A) and Świdnik IG 1, consists mainly of psammitic compact volcanic glass and pumice. The tuffs formed due to pyroclastic eruptions of at least two volcanoes in the NE and central areas of the basin. The decompacted tuff thickness of ca. 9–16 m indicates deposition a few kilometres from the eruption site (cf. Segerstrom 1950; Francis and Oppenheimer 2004). The tuffs in the NE area have the same age as the overlying basalt flows of element VII.2, whereas the tuffs in the central area are slightly older than the overlying basalt flow.

The effusive element VII.2 was recognized in the NE, central and SW areas. These rocks are alkaline basalts formed due to the activity of at least two volcanic cones. In the NE area (borehole Parczew IG 10), two lava-flows have been identified – an older one and a younger one (Text-fig. 15A), whereas in the central and SW areas, there is a single lava-flow – the younger one. Basalts have the greatest thickness of 22–24 m in boreholes Parczew IG 10 and Świdnik IG 1. In borehole Niedrzwica IG 1, their thickness is only 2 m, but might have been originally greater and subsequently reduced by erosion during the next BSL fall.

The volcanic activity evidenced by thick basalts probably formed a morphological elevation in the NE area, as suggested by Skompski (2011), and in the central area. Each of the volcanoes was presumably located several kilometres away from the Parczew IG 10 and Świdnik IG 1 boreholes, respectively. The distance was estimated based on the thickness and type of lava according to the coefficient value given by Walker (1973). The effect of this elevation as a morphologic element is shown by the specific, highly reduced section of sequences 2 and 3 in borehole Parczew IG 10 (Text-fig. 16).

No effusive volcanic rocks have thus far been reported from the SE area. However, petrographic studies identified a volcanic rock in borehole Terebin IG 3, described in the borehole final report as siltstone passing into kaolinite claystone containing iron spherulites. It is a highly altered volcanic rock consisting of kaolinite and hematite that were formed by the alteration and replacement of probably acidic volcanic glass, as evidenced by the presence of perlitic texture (cf. Siemaszko 1978; Ryka and Maliszewska 1991; Rottella and Simandl 2004; Al-Mashaikie and Al-Hawbanie 2010). The rock contains also single quartz grains, and its composition differs considerably from that of basalts related to alkaline lavas in the other areas. This evidence of volcanic rock in the SE area indicates that an active volcanic cone existed in this area as well.

Unpreserved TST and HST

The whole sequence 1 in the investigated borehole sections consists of alluvial deposits, with no recognizable surfaces of transgression and maximum flooding that would be bounding the TST and HST of the sequence. Only the surface of forced regression could be put hypothetically at the erosional base of the sequence to indicate maximum regression. There are no recognizable marine and deltaic deposits that would represent the TST and HST in a classical sequence model.

However, deposits of that type are described from two other borehole sections located between the studied areas of the Lublin Basin (Text-fig. 1). The recognizable TST and HST of sequence 1 in these boreholes are represented by deposits of shallow-marine clayey shelf, carbonate shelf and prodelta, with a maximum thickness of ca. 70 m in borehole Ruskie Piaski IG 2 (Kozłowska and Waksmundzka 2020). The succession in borehole Busówno IG 1 is thinner, but its lithofacies are similar. The two boreholes are considered to show the erosional relics of TST and HST that escaped truncation by the basal forced-regression surface of sequence 2 due to the differential basin subsidence. The HST and TST in the investigated borehole sections were apparently removed by this next episode of forced regression. Deep erosional truncation of the topmost part of LST, probably including basalts, is observed in borehole Lublin IG 1, where it was related to the formation of an incised valley (FRST) of sequence 2.

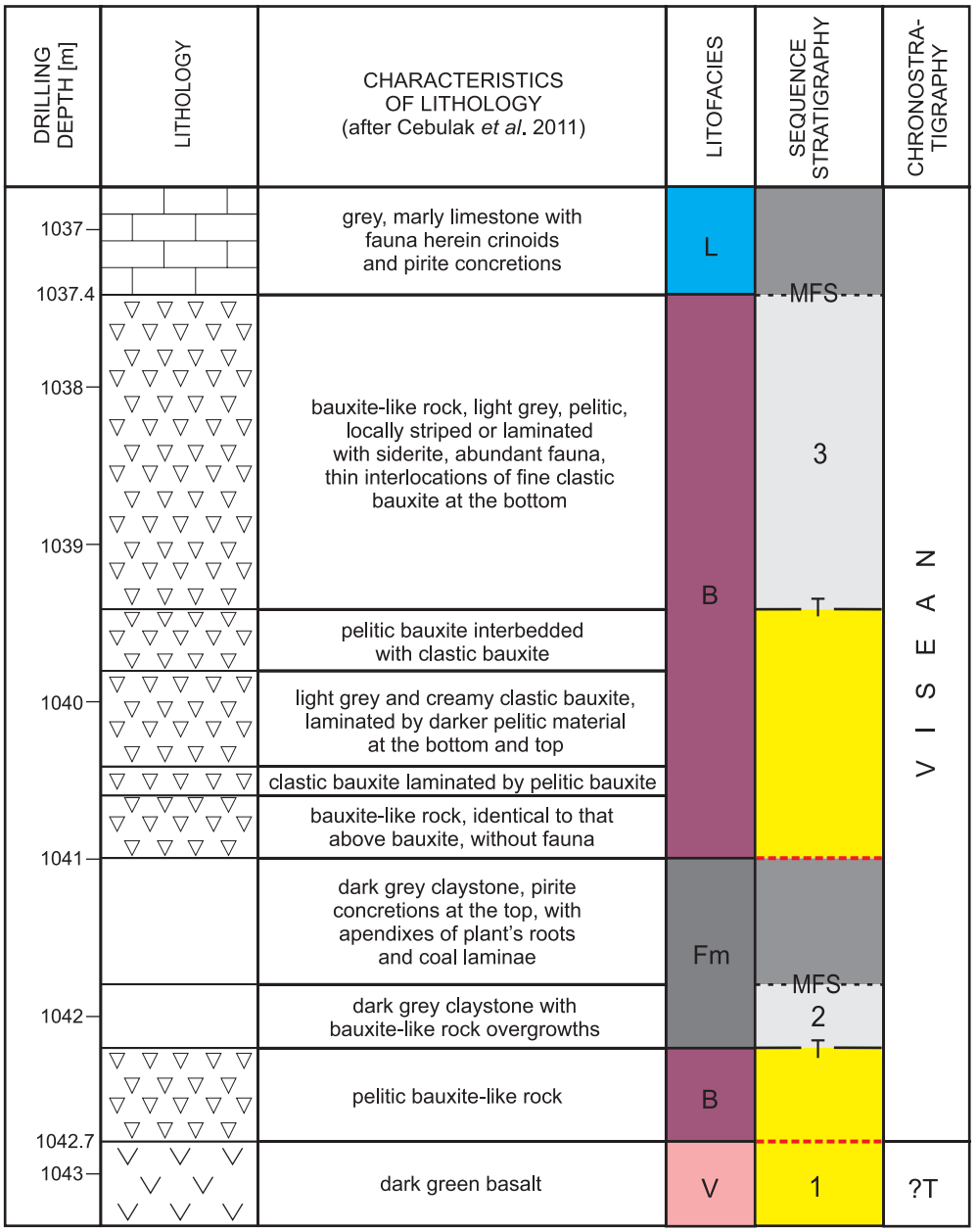

Text-fig. 16. Lithology, lithofacies, depositional environments and sequence stratigraphy of bauxites, bauxite-like rocks and associated deposits in the NE area of the Lublin Basin, based on examples in borehole Parczew IG 10; ?T – putative Tournaisian; for further explanation, see Text-fig. 6.

Sequence 2

The present-day thickness of sequence 2 (Text-fig. 14A) is much greater than that of sequence 1, except in the NE area and borehole Świdnik IG 1, where it is clearly reduced due to the basalt updoming. The greatest thickness of this sequence, ca. 100 m, is in the SE area (borehole Korczmin IG 3).

FRST and LST

The base of sequence 2 is an erosional surface that developed during the next major fall of base level (FRST). In the area of borehole Lublin IG 1, this erosion resulted in a large incised valley, ca. 25 m deep, that probably trended towards the SW (borehole Niedrzwica IG 1). During the base-level lowstand

and slow initial rise, the valley was filled mainly with the fluvial lithofacies of massive sandy conglomerates GSm, gravelly sandstones SGm and sandstones Sm, deposited in gravel-bed braided channels as a result of hyperconcentrated flows (cf. Waksmundzka 2010a). The LST shows fining-upward cyclothems, predominantly of type IIa and sporadically of type I.

In the NE area (borehole Radzyń IG 1), a smaller incised valley developed, ca. 4 m deep (Text-fig. 15B). In the SE area, shallow braided channels were incised to a depth of ca. 1 m. The fluvial erosion of FRST took place not only in the area of borehole Terebin IG 3, where volcanites of sequence 1 occur as substrate, but may have also formed small morphological elevations that became areas of non-deposition during the lowstand, as in the area of borehole Świdnik IG 1. In the area of borehole Parczew IG 10, a bauxite-like deposit formed in terrestrial conditions due to the chemical weathering of an underlying basalt (Text-fig. 15B). In the area of borehole Kock IG 2, no fluvial channels developed, but only a thin layer of mudstones was deposited on a floodplain at the climax of TST. The erosional FRST thus created a highly diversified land topography, which was gradually buried by the LST and TST sedimentation.

As to volcanic signatures, the valley extending from the area of borehole Radzyń IG 1 was filled with massive quartz arenites Sm in its lower part and with tuffs in the upper part. The tuffs contain detrital and volcanic quartz, rhyolite, pumice and altered volcanic glass. Similar components, supplemented with basalt grains, occur in the valley-fill polymictic paraconglomerates in the Lublin-Niedrzwica area and in the channel-fill in borehole Zubowice IG 5, where no basalt detritus is observed, but feldspars are present.

TST and HST

The FRST drainage system of incised valleys and river channels was filled in by the LST fluvial deposits. The TST sedimentation then occurred and culminated in the deposition of claystones, mudstones and *Stigmaria* soils in a coastal floodplain environment, with a maximum original (decompacted) thickness of ca. 25–33 m in the central and SW areas of the basin. The LST/TST transition is a transgression surface, above which in most borehole sections are the early transgressive deposits. These are predominantly claystones and mudstones deposited in the environments of prodelta and delta front of a shallow-marine delta system in the former land areas.

In the SE area, the upper TST section shows deltaic deposits interfingering with limestones and marls deposited on a shallow carbonate shelf, and with claystones of a shallow muddy shelf. This is an area of the greatest thickness of the TST deposits, which indicates the largest accommodation space, with the basin-fill showing non-gradational cyclothems IIIc (Waksmundzka 2013). The abundance of carbonate layers indicates that the TST in this part of the basin was most invasive and involved the most distal, open-marine depositional environment. Sedimentation in the other areas took place chiefly in a shallow-marine delta environment, with a much smaller accommodation space. The lithofacies of parasequences, the coarsening-upward cyclothems Ic, IIc and non-gradational cyclothems IIIc, indicate predominantly aggradation with minor progradation. Deltaic depositional regime prevailed, and the sedimentation on a shallow carbonate shelf occurred only in the SW area. This evidence suggests that the marine transgression (TST) of sequence 2 encroached into the Lublin Basin in the late Visean from the south. The decompacted thickness of cyclothems Ic (borehole Lublin IG 1) indicates that the depth of the marine basin increased from ca. 30 to ca. 130 m.

The least accommodation space was created in the NE area, where the TST deposits have a highly reduced thickness. In the area of borehole Radzyń IG 1, a few metres of prodelta sediment were originally deposited, while in the area of borehole Kock IG 2 – ca. 2 m of flora-containing mudstones accumulated very likely on a flooded delta plain. In the area of borehole Parczew IG 10 (Text-fig. 16), a flooded delta plain formed upon the lava-flow basalt due to the base-level rise (TST). A lake developed in this area, first accumulating claystone with interbeds of bauxite-like rocks and then, in the HST, claystones with plant-root traces and coal laminae. The lake was thus filled with deposits and covered by vegetation.

At the top of the TST, there is a maximum flooding surface that runs within the claystones and mudstones of the shallow clayey shelf, which are characterized by an increased radioactivity manifested by a maximum on gamma-ray logs (boreholes Niedrzwica IG 1, Lublin IG 1 and Kock IG 2). This surface is overlain by HST deposits lithologically similar to those of the above-described TST, accumulated in analogous depositional environments.

Sequence 3

FRST and LST

The present-day (compacted) thickness of sequence 3 is smallest, ca. 15–60 m, in the NE area and

increases to ca. 150–200 m towards the central, SW and SE areas. The base of the sequence is a regional discontinuity (FRST) with redeposited, allochthonous bauxites, overlain by bauxite-like lacustrine deposits (LST) in boreholes Parczew IG 10 and Radzyń IG 1 (Text-figs 15C, 16).

TST and HST

In the NE area, a relatively small accommodation space was created for marine transgression by the base-level rise (TST). In borehole Kock IG 2, the accommodation was slightly larger and allowed deposition of numerous carbonate beds. In borehole Radzyń IG 1, the TST includes a delta distributary channel that formed probably due to an erosional-depositional event caused by local tectonism. The channel-fill sandstone contains clasts of andesite, basalt, pumice, rhyolite and volcanic glass, similar to those found in sequences 1 and 2. In borehole Parczew IG 10, bauxite-like lacustrine deposits continued to form in the TST, but as the transgression proceeded – the area became inundated by the sea, allowing shallow-marine carbonate shelf sedimentation. The maximum flooding surface is placed at the first carbonate bed deposited at that time.

In borehole Radzyń IG 1, this limestone bed contains what is probably lapilli-type pyroclastic material of basalt/andesite-type volcanic rocks. It was likely transported to the shallow carbonate shelf by air, after being expelled from the crater of a nearby active volcano, whose cone was rising above the sea level. Another possibility is that these volcanic clasts were derived by erosion during the marine transgression of sequence 3, since there is no evidence of volcanic activity above the limestone bed.

The HST overlying this limestone bed is a parasequence composed of the coarsening-upward cyclothems Ic and IIc and non-gradational cyclothems IIIc. In the area of borehole Parczew IG 10, the marine basin was relatively shallow, ca. 27 m deep, deepening towards the SW, S and SE.

Sequence 4

FRST and LST

The present-day (compacted) thickness of sequence 4 varies from ca. 17–40 m in the NE and NW areas, through ca. 75 m in the central area, to a maximum of 110 m in the SE area.

The FRST comprises moderate incised valleys and interfluve *Stigmaria* palaeosoils. The LST deposits of the NE area are highly varied. The small incised valley, ca. 10 m deep, in borehole Radzyń IG 1 was filled with planar-stratified gravelly sandstones of lithofacies SGh. These are quartz arenites containing clasts of volcanic quartz, feldspar, quartz shale and sandstone. The sandstones are overlain by floodplain deposits whose original thickness could reach ca. 22 m. At the top of these deposits is the surface of initial transgression, representing the LST/TST boundary. This surface probably correlates with the top of *Stigmaria* mudstones (R) deposited on a delta plain in borehole Parczew IG 10. The palaeosoils mudstones have a thickness of ca. 1 m and represent condensed FRST-LST. The shoreline of the marine basin was probably slightly further towards the SW, as indicated by the section of sequence 4 in borehole Kock IG 2, where the LST and HST are deposits accumulated on a shallow-marine delta slope.

TST and HST

The sedimentation during transgression (TST) and highstand (HST) involved prodelta and delta slope claystones and mudstones, as well as shallow shelf limestones and marls. The maximum flooding surface runs at the base of a carbonate bed that is clearly thicker in the area of borehole Parczew IG 10. Detailed microfacies analysis of carbonate beds from the Parczew area was presented by Skompski (1996, 2011), indicating deposition in a shallow marine environment.

DISCUSSION

Sequence stratigraphy vs. chronostratigraphy

The sequence stratigraphy in the present study (Text-fig. 2) has been tied to the Carboniferous global division (Davydov *et al*. 2012) and Western European subdivision (Ramsbottom 1977, 1978). This general correlation is based on precisely dated goniatites (Musiał and Tabor 1979, 1988), conodonts (Skompski and Soboń-Podgórska 1980; Skompski 1996, 1998) and foraminifers (Skompski and Soboń-Podgórska 1980; Soboń-Podgórska 1988; Soboń-Podgórska and Tomaś 1995), and on flora investigations (Migier 1988; Kmiecik 1988) within the part of the Carboniferous succession comprising sequences 2–22 (Waksmundzka 2008, 2010a, 2013; Kozłowska and Waksmundzka 2020). Biostratigraphic and palynological data concerning the age of sequences 2–4 were also considered for the Upper Visean in the

investigated borehole sections (Korejwo and Teller 1968, 1972; Żelichowski 1972; Korejwo 1974, 1986; Bojkowski and Musiał 1978; Musiał and Tabor 1989; Kmiecik and Trzepierczyńska 2007; Woszczyńska 2011).

The oldest part of the succession, sequence 1, was earlier included into the Visean, but requires revision, because the new dating of basalts in its element VII.2 in the NE area of the Lublin Basin indicates an older age, corresponding to the Late Tournaisian (Pańczyk and Nawrocki 2015). The new isotopic dating of basalts puts into question their Late Visean age suggested previously by Depciuch (1974), Porzycki (1988) and Grocholski and Ryka (1995), while supporting the earliest suggestions of a Tournaisian–early Visean? age by Miłaczewski and Niemczycka (1967) and by Korejwo and Teller (1972). Notably, volcanic and/or pyroclastic rocks are known from the middle and upper Tournaisian in several other areas in Poland (Szulczewski *et al*. 1996; Muszyński *et al*. 1996; Matyja 2008; Godyń 2011; Narkiewicz 2020).

Therefore, the age of the underlying elements I–VI and VII.1 of sequence 1, covering the pre-Carboniferous bedrock, cannot be younger than the putative late Tournaisian age of element VII.2. The suggestion of a Tournaisian age of the fluvial deposits underlying the basalts in the NE area of the Lublin Basin was first put forward by Pańczyk and Nawrocki (2015). This notion is supported further by a comparison with the oldest part of the Carboniferous succession in the nearby Lviv-Volyn Basin in Ukraine, where it is dated to the Late Tournaisian based on biostratigraphic data (Shulga *et. al*. 2007; Kostyk *et al*. 2016). This part of the section therein, called the Khoriv suite, is bounded by erosional surfaces at the base and top (Shulga *et. al*. 2007), in a similar manner to sequence 1 in the Lublin Basin. Claystones, mudstones, sandstones and conglomerates occur in the lower part of the Khoriv suite, while the upper part is composed of limestones and dolomites (Kostyk *et al*. 2016). However, the lithology is variable, because carbonates are not found everywhere and the thickness varies from 10–35 m to 70–313 m in various parts of the Lviv-Volyn Basin. The sequence 1 in the Lublin Basis is most similar to the Khoriv suite section in the Novovolins"k and Chervonograd areas adjacent to the state border at the SE extension of the Lublin Basin.

Considering the isotopic age 348.2 ± 0.8 Ma (Pańczyk and Nawrocki 2015) of the basaltic element VII.2 at the top of sequence 1 and the Tournaisian eustatic trend (after Davydov *et al*., 2012), it is possible that the LST/TST boundary in this sequence corresponds to the surface Tour2, which has an approximate age of about 349 Ma and marks the onset of a transgressive trend that lasted until the end of the Tournaisian. However, this working hypothesis requires confirmation by further research, because the HST and TST of sequence 1 are not preserved, being eroded in the investigated borehole sections. If the hypothesis is correct, the unconformity between sequences 1 and 2 would then correspond to the Tournaisian/Visean boundary and include a stratigraphic gap spanning the uppermost Tournaisian and the lower to middle Visean (Text-fig. 2). The same age of erosional processes in the Lublin Basin is postulated by Narkiewicz (2020) and an analogous stratigraphic gap is observed in the Lviv-Volyn Basin (Kostyk *et al*. 2016).

Comparison of the lithostratigraphic boundaries of the Kłodnica Member and its sequence stratigraphy in the studied sections indicates considerable variation in the time span of this member within the basin (Text-fig. 2). In the NE area, the member corresponds to sequences 1 and 2 and the lower part of sequence 3, except in borehole Kock IG 2 (Text-fig. 6). In the central and SW areas, it correlates with sequence 1 or its lower part (Text-fig. 7), whereas in the SE area – with sequence 1 and the lowermost part of sequence 2 (Text-fig. 8). Consequently, it can be assumed that the deposits of the member in the NE and SE areas accumulated in the late Tournaisian to early late Visean, and that a stratigraphic gap occurs within the member. However, the deposition of the Kłodnica Member in the central and SW areas and in the area of borehole Kock IG 2 occurred only in the late Tournaisian and formed there the oldest part of the Carboniferous succession in the basin.

Accommodation space, transport directions and source areas

The analysis of decompacted thickness variation indicates that during the formation of the LST of sequence 1 (Text-fig. 14A), in the late Tournaisian, the depocentre was in the central area (borehole Lublin IG 1) of the Lublin Basin. It was the area of highest subsidence, where the greatest accommodation space was created and where predominantly aggradation of floodplain deposits occurred (Text-fig. 12). Large accommodation space existed also in the SW area, where strong aggradation of floodplain, braided-river and hyperconcentrated flow deposits occurred in the incised valleys. The high subsidence in the central and SW areas and low subsidence in the NE area produced a topographic gradient that effectively ren-

dered the SW transport direction dominant in the Lublin Basin.

The formation of incised valleys might have been predisposed in areas where the bedrock was cut by faults. A sub-Carboniferous palaeogeological map of the Lublin Basin (Miłaczewski 2010) shows that one of the dominant trends of these faults is SW-NE, and this might have been the general direction of the incised valleys. Narkiewicz (2020) indicates some of these faults as being active during the Devonian and their location is similar to the suggested directions of the incised valleys (Text-fig. 13).

According to a new interpretation of seismic data, some faults in the NE part of the Lublin Basin have a W-E trend (Tomaszczyk and Jarosiński 2017). If they existed in the late Tournaisian, within the eroded bedrock of the incised valleys, they would have also influenced the direction of the latter. Assuming the SW palaeotransport direction as dominant, the hanging walls of the W-E faults might have given rise to a transverse relief variation that modified both the morphological gradient and the depth of the valley incision. The folds and thrusts of the Kock Zone, as well as the faults in the Lublin-Niedrzwica area, were also transverse to the palaeotransport direction.

The small palaeothickness of sequence 1 in the SE area increases from the NE towards the SW and S, generally in the same direction as in the remaining areas. The smallest palaeothickness is found in the area of boreholes Terebin IG 2 and Terebin IG 3, where there were probably lava-flows forming morphological highs. In contrast, subsidence was higher in the area of boreholes Zubowice IG 5 and Korczmin IG 1, where aggradation of terminal floodplain deposits took place.

Except for the presumed Devonian substrate clasts found at its bottom, the valley fill of element I contains clastic components that may have been derived from the areas of weathered volcanic, crystalline and pre-Carboniferous sedimentary rocks exposed to the NE, in the area of Łuków-Wisznice Elevation (Text-fig. 13). The grains of granitoids, granodiorites, feldspars, detrital quartz, basalts and quartz arenites may have originated from that area. The remaining clasts represent rocks other than basalts, such as andesites and acidic volcanic rocks (rhyolites), and these were derived probably from another area. The likely second extensive source areas for this clastic material were the weathering outcrops of Precambrian rocks to the NE and E, in the Volynian Polesia (Text-fig. 13). Among the other clastic components, there are granitoids, with xenoliths of acidic effusive rocks, and volcanic rocks of basalt-rhyolite and andesite-dacite type (Nosowa *et al*. 2005; Shumlyanskyy 2014; Wiszniewska and Tołkanowicz 2015). The volcaniclastic rocks described by Godyń (2011) from the Tournaisian succession in Western Pomerania are similarly composed of grains of acidic volcanic rocks such as rhyolites-dacites.

The basalt clasts might have thus come from these two source areas, while the clasts of acid rocks – from the farther Polesia source only. This suggestion about the source areas for basalt clasts is justified by the established chronology of the depositional elements of sequence 1 and volcanic processes, as this evidence implies that the basalts of element VII.2 are the youngest rocks of sequence 1 in the study area and hence could not have been subject to erosion during the deposition of element I.

It seems that the sediment transported by braided rivers and filling the incised valley (elements III and V) in the NE, central and SW areas was derived from the same source terranes as that supplied for the early valley fill of element I. There are some locally derived Silurian claystone clasts in the incised valley fill in the NE area and Devonian sandstone clasts in the SW area. In contrast, only clasts derived most probably from the local Devonian quartz arenite bedrock occur in the area of boreholes Kock IG 2 and Korczmin IG 3, in similar fashion to the occurrence of locally derived carbonate rock clasts in borehole Korczmin IG 1. This local variation in sediment composition supports the notion of a fluvial drainage system cutting through a tectonically created, varied morphological relief of the basin floor, with transverse substrate faults and folds.

The clastic components of elements I, III and V include volcanic glass, the origin of which is difficult to determine unequivocally. This detritus comes probably from the strong fragmentation of sediment containing volcanic rock fragments transported through the incised valleys. Another source, so far unconfirmed by borehole sections, could be a pyroclastic supply by contemporaneous volcanic eruptions. The age of contemporaneous tuffs thus far documented (element VII.1 in sequence 1 and LST of sequence 2) is younger. Therefore, contemporaneous volcanic activity in the basin during the deposition of elements I, III and V of sequence 1 remains a speculative possibility and be a focus of future research.

Spatial analysis of the decompacted thickness of sequence 2 (Text-fig. 14B) suggests that the early late Visean sedimentation in the NE area occurred under very low subsidence and accommodation. In contrast, the subsidence in the central and SW areas

was higher, because the depocentre clearly expanded towards the SE. The maximum palaeothickness of more than 290 m is in borehole Korczmin IG 3. The differential subsidence created a topographic gradient that directed the fluvial drainage towards the SW, S and SE. The accommodation space in the central and SW areas was initially filled by deposits of braided rivers and hyperconcentrated flows within incised valleys, succeeded by aggradation of a terminal floodplain.

The course of the incised valleys of sequence 2 might have been generally similar to that of the valleys of sequence 1. The sediment supply of LST failed to keep pace with an increasing subsidence, which gave rise to a marine transgression and deposition on a shallow carbonate and clayey shelf (TST) and deposition of aggrading-prograding deltaic lobes (HST). The greatest accommodation space was created in the SE area. A similar, SE-ward bedrock inclination was recognized by Środoń *et al*. (2013) of the Lviv-Volyn Basin in Ukraine, at the extension of the Lublin Basin.

The compositional characteristics of volcaniclastic conglomerates and sandstones of sequences 1–4 indicate that the majority of sediment components came from outside of the Lublin Basin and only few have their source in the pre-Carboniferous substrate. In the NE area (borehole Radzyń IG 1), the lower part of the incised valley (FRST) of sequence 2 was filled (LST) with quartz arenites in the earliest late Visean. This is a mineralogicaly mature sediment, indicating that – for the first time since the onset of Carboniferous sedimentation – the basin's fluvial drainage system in the early late Visean began to receive rock detritus from undefined distant sources, as compared to sequence 1. The upper part of the valley fill, in turn, consists of tuffs containing components which are similar to those found in the elements I, III and V of sequence 1 and which may have originated from the same sources, including local pyroclastic eruptions in the NE area of the basin.

In the NE area (borehole Radzyń IG 1), the TST of sequence 3 includes a delta-plain distributary channel that was formed during the middle late Visean and reflects an imbalance of the fluvial drainage overpowering the base-level rise due to local tectonism. Its sandstone infill contains clasts lithologically similar to those found in sequences 1 and 2, and hence originating probably from the same sources. In the same area, the incised valley (FRST) of sequence 4 is filled (LST to TST) with quartz arenites. It can thus be concluded that, already in the latest late Visean, the source areas ceased to supply the clastic components that dominated in sequences 1–3 (i.e. acidic and alkaline volcanic rock detritus), and – with an expansion of the fluvial drainage – a supply of sediment from other, undetermined distant source areas commenced in the basin.

CONCLUDING REMARKS

- The oldest part of the Carboniferous succession in the Lublin Basin, known as the Kłodnica Member of the Huczwa Formation, has been investigated through lithofacies analysis, sequence stratigraphy and petrographic studies. The focus was on sedimentary palaeoenvironments, cyclothems (i.e. parasequences) and stratigraphic sequences based on the vertical organization of lithofacies associations, forced-regression surfaces, transgression and maximum flooding surfaces, with the distinction of forced-regressive, lowstand, transgressive and highstand systems tracts.
- According to a sequence stratigraphy model established for the Lublin Basin, the Kłodnica Member comprises sequences 1–3 in the basin NE area and sequences 1–2 in its remaining areas. The study gives special attention to sequence 1, as the oldest Carboniferous deposits in the basin.
- Chronostratigraphic correlations and comparison with the Khoriv suite in the adjacent Lviv-Volyn Basin in Ukraine, together with the isotopic age of basalts and biostratigraphic and palynological data, indicate that the putative upper Tournaisian in the Lublin Basin corresponds to sequence 1, whereas sequences 2–4 represent the upper Visean. A stratigraphic gap, spanning the uppermost Tournaisian and the lower to middle Visean, occurs between sequences 1 and 2.
- The fining-upward cyclothems of type I and the lower parts of the cyclothems of type IIa were deposited mainly by hyperconcentrated flows and in shallow braided river channels within incised valleys. Deposition of the upper parts of the cyclothems of type IIa and IIb took place on a terminal alluvial floodplain. The coarsening-upward cyclothems of type Ic and IIc formed mainly in a delta environment and subordinately on a shallow-marine carbonate to clayey shelf. Non-gradational cyclothems of type IIIc formed in the distal carbonate/clayey shelf and prodelta environments.
- The dominant direction of fluvial drainage in the Lublin Basin was towards the SW. The facies associations, evolution of depositional environments and lateral thickness variation of the studied de-

posits were controlled by a combination of eustatic changes and basin-floor differential tectonic subsidence.

- The Carboniferous deposits of sequence 1 represent the FRST and LST, with the HST and most of TST not preserved due to subsequent erosion by the FRST of sequence 2. These deposits, recording the formation of incised valleys (FRST) followed by fluvial aggradation during the early base-level rise (LST), are divided into a chronological succession of architectural elements I–VII.1–2. Elements I, III and V are fluvial conglomerates and coarse-grained sandstones, whereas the mud-dominated elements II, IV and VI are deposits of a limnic terminal floodplain that developed within the LST. The stratigraphic alternation of fluvial and limnic elements in the LST reflects temporal deficit of the basin accommodation space.
- The volcaniclastic deposits of elements I, III and V are polymictic paraconglomerates, lithic/sublithic to subarkose arenites and sublithic wackes, containing grains of acidic and alkaline volcanic and igneous rocks. Their mineral composition indicates sediment derivation from the weathered outcrops of volcanic, crystalline and pre-Carboniferous sedimentary rocks located to the NE and E of the Lublin Basin, in the areas of Łuków-Wisznice Elevation and Volynian Polesia. Sediment was also locally derived from intrabasinal tectonic elevations of Devonian bedrock crosscut by rivers.
- Elements VII.1 (pyroclastic) and VII.2 (volcanic) record an episode of volcanism in the basin, dated to the late Tournaisian. The volcanic rocks represent alkaline lava-flows in the central and SW parts of the basin, and acidic lava-flows in the SE part.
- The overlying Visean sequences 2–4 similarly comprise fluvial-lacustrine FRST and LST, and TST and HST deposited in shallow-marine clayey/carbonate shelf, prodelta and deltaic environments.
- Based on sequence-stratigraphic analysis, the study concludes that the lithostratigraphic boundaries of the Kłodnica Member of the Huczwa Formation are highly diachronous, controlled by the tectonic topography and differential subsidence of the Lublin Basin.

Acknowledgements

Our gratitude is to Stanisław Skompski for his help, fruitful discussions and many useful suggestions. Hanna Matyja kindly helped with consultations. We are grateful to Krystian Wójcik for his help with the editing of the manuscript and to Anna Becker for helpful discussions. Special thanks go to Bogusław Waksmundzki for drawing the block diagrams. SEM and EDS analysis was performed by Leszek Giro. The authors are grateful to the reviewers Wojciech Nemec and Andrzej Muszyński for all suggestions and corrections. The project was conducted at the Polish Geological Institute – National Research Institute and financed by the Ministry of Science and Higher Education (No. 61.2801.1301.00.0, No. 62.9012.2044.00.0). The research work was carried out at the Archives of Drilling Cores and Geologic Samples of the National Geological Archive in Iwiczna near Piaseczno and in Hołowno.

REFERENCES

Al-Mashaikie, S.Z.A.K. and Al-Hawbanie, A.M. 2010. Petrography and geochemical study of the Perlite Rocks from Bait Al-Qeyarie, Kawlan Area, Yemen. *Earth Science*, **21** (2), 195–217.

Arnott, R.W.C and Hand, B.M. 1989. Bedforms, primary structures and grain fabric in the presence of suspended sediment rain. *Journal of Sedimentary Petrology*, **59** (6), 1062–1069.

Ashley, G.M. and Sheridan, R.E. 1994. Depositional model for valley fills on a passive continental margin. In: Dalrymple, R.W., Boyd, R. and Zaitlin, B.A. (Eds), Incised-Valley Systems: Origin and Sedimentary Sequences. *Society of Economic Paleontologists and Mineralogists Special Publication*, **51**, 285–301. Tulsa, Oklahoma.

Baldwin, B. and Butler, C.O. 1985. Compaction Curves. *American Association of Petroleum Geologists Bulletin*, **69** (4), 622–626.

Batalla, R.J., De Jong, C., Ergenzinger, P. and Sala, M. 1999. Field observations on hyperconcentrated flows in mountain torrents. *Earth Surface Processes and Landforms*, **24**, 247–253.

Bojkowski, K. and Dembowski, Z. 1988. Paleogeography of Carboniferous in the Lublin Coal Basin at the background of paleogeography of Carboniferous in Poland. In: Dembowski, Z. and Porzycki, J. (Eds), Carboniferous of the Lublin Coal Basin. *Prace Instytutu Geologicznego*, **122**, 18–26; 227–228.

Bojkowski, K. and Musiał, Ł. 1978. Stratygrafia makrofaunistyczna karbonu. In: Niemczycka, T. (Ed.), *Profile Głębokich Otworów Wiertniczych Instytutu Geologicznego*, **45**, 129–131.

Catuneanu, O. 2006. Principles of Sequence Stratigraphy, 375 pp. Elsevier; Amsterdam.

Cebulak, S. 1988a. Petrographic characteristics of Carboniferous deposits. In: Dembowski, Z. and Porzycki, J. (Eds), Carboniferous of the Lublin Coal Basin. *Prace Instytutu Geologicznego*, **122**, 77–88; 231–232. [In Polish with English summary]

Cebulak, S. 1988b. Geological outline of sub-Carboniferous

basement. In: Dembowski, Z. and Porzycki, J. (Eds), Carboniferous of the Lublin Coal Basin. *Prace Instytutu Geologicznego*, **122**, 31–34. [In Polish with English summary]

Cebulak, S. 1989. Badania petrograficzne osadów karbonu. In: Krassowska, A. (Ed.), *Profile Głębokich Otworów Wiertniczych Państwowego Instytutu Geologicznego*, **66**, 180–189.

Cebulak, S., Porzycki, J., Laskowski, M., Różkowski, A., Rudzińska, T., Szewczyk, J., Karwasiecka, M. and Waksmundzka, M.I. 2011. Badania surowcowe boksytów i węgli występujących w utworach karbonu. In: Pacześna, J. (Ed.), *Profile Głębokich Otworów Wiertniczych Państwowego Instytutu Geologicznego*, **130**, 116–122. [In Polish with English summary]

Coleman, J.M. and Wright, L.D. 1975. Modern river deltas: variability of processes and sand bodies. In*:* Broussard, M. L. (Ed.), Deltas, models for exploration, 99–150*.* Houston Geological Society; Houston.

Davydov, V.I., Korn, D. and Schmitz, M.D. 2012. The Carbonifeous Period. In: Gradstein, F.M., Ogg, J.G., Schmitz, M.D. and Ogg, G.M. (Eds), The Geologic Time Scale, 603–651. Elsevier, Amsterdam.

Depciuch, T. 1974. Rocks of the Precambrian Platform in Poland. Part 2 – Sedimentary cover. In: Łaszkiewicz, A. (Ed.), *Prace Instytutu Geologicznego*, **74**, 81**–**83. [In Polish with English summary]

Duff, McL.D. and Walton, E.K. 1962. Statistical basis for cyclothems: a quantitative study of the sedimentary succession in the East Pennine Coalfield. *Sedimentology*, **1** (4), 235–255.

Einsele, G. 1992. Sediment of Marine Delta Complexes, Depositional Rhythms and Cyclic Sequences. In: Einsele, G. (Ed.), Sedimentary Basins. Evolution, Facies and Sediment, 147–160; 271–310. Springer-Verlag; Berlin, Heidelberg.

Elliott, T. 1974. Interdistributary bay sequence and their genesis. *Sedimentology*, **21** (4), 611–622.

Elliott, T. 1975. The sedimentary history of a delta lobe from a Yoredale (Carboniferous) cyclothem. *Proceedings of the Yorkshire Geological Society*, **40** (4), 505–536.

Elliott, T. 1976a. Sedimentary sequences from the Upper Limestone Group of Northumberland. *Scottish Journal of Geology*, **12** (2), 115–124.

Elliott, T. 1976b. Upper Carboniferous sedimentary cycles produced by river-dominated, elongate deltas. *Journal of the Geological Society of London*, **132**, 199–208.

Elliott, T. 1978. Deltas. In: Reading, H.G. (Ed.), Sedimentary envinronments and facies, 97–142. Blackwell Scientific Publications; Oxford.

Fisher, R.V. and Schmincke, H.U. 1984. Pyroclastic rocks, 471 pp. Springer-Verlag; Berlin, Heidelberg, New York, Tokyo.

Flügel, E. 2004. Depositional Models. Facies Zones and Standard Microfacies. In: Flügel, E. (Ed.), Microfacies of Carbonate Rocks Analysis, Interpretation and Application, 657–723. Springer-Verlag; Berlin, Heidelberg.

Francis, P. and Oppenheimer, C. 2004. Volcanoes, 536 pp. Oxford University Press; Oxford.

Galets'kyi, L.S. 2007. An Atlas of the Geology and Mineral Deposits of Ukraine 1:5 000 000. Section IV. Geological slice maps: Pre-Carboniferous. National Academy of Science of Ukraine; Kyiv and Toronto.

Gastaldo, R., Denko, T. and Liu, Y. 1993. Application of sequence and genetic stratigraphic concepts to carboniferous coal-bearing strata: an example from the Black Warrior Basin, USA. *Geologische Rundschau*, **82** (2), 212–226.

Godyń, K. 2011. Volcaniclasts of Lower Carboniferous rock formations in Western Pomerania. *Biuletyn Państwowego Instytutu Geologicznego*, **444**, 55–64. [In Polish with English summary]

Grocholski, A. and Ryka, W. 1995. Carboniferous magmatism of Poland. In: Zdanowski, A. and Żakowa, H. (Eds), The Carboniferous System in Poland. *Prace Państwowego Instytutu Geologicznego*, **148**, 181–190.

Hajdenrajch, M. 2010. Stratygrafia sekwencji i sedymentacja utworów karbonu rejonu Niedrzwicy (płd.-zach. Lubelszczyzna), 68 pp. Unpublished M.Sc. thesis, University of Warsaw; Warszawa.

Hampson, G., Stollhofen, H. and Flint, S. 1999. A sequence stratigraphic model for the Lower Coal Measures (Upper Carboniferous) of the Ruhr district, north-west Germany. *Sedimentology*, **46** (6), 1199–1231.

Hein, F.J. and Walker, R.G. 1977. Bar evolution and development of stratification in the gravelly, braided, Kicking Horse River, British Columbia. *Canadian Journal of Earth Sciences*, **14** (4), 562–570.

Helland-Hansen, W. 2009. Towards the standardization of sequence stratigraphy. *Earth-Science Reviews*, **94**, 95–97.

Helland-Hansen, W. and Gjelberg, J.G. 1994. Conceptual basis and variability in sequence stratigraphy: a different perspective. *Sedimentary Geology*, **92** (1–2), 31–52.

Jaworowski, K., 1987. Kanon petrograficzny najczęstszych skał osadowych. *Przegląd Geologiczny*, **35** (4), 205–209.

Kędzior, A., 2016. Reconstruction of an Early Pennsylvanian fluvial system based on geometry of sandstone bodies and coal seams: the Zabrze Beds of the Upper Silesia Coal Basin, Poland. *Annales Societatis Geologorum Poloniae*, **86** (4), 437–472.

Kmiecik H., 1988. Miospore stratigraphy of the Carboniferous deposits. In: Dembowski, Z. and Porzycki, J. (Eds), Carboniferous of the Lublin Coal Basin. *Prace Instytutu Geologicznego*, **122**, 131–141; 235–237. [In Polish with English summary]

Kmiecik, H. and Trzepierczyńska, A. 2007. Wyniki badań palinologicznych utworów karbonu. In: Waksmundzka, M.I. (Ed.), *Profile Głębokich Otworów Wiertniczych Państwowego Instytutu Geologicznego*, **119**, 119–126. [In Polish with English summary]

Korejwo, K. 1974. The Carboniferous of the Abramów structure. *Acta Geologica Polonica*, **24** (4), 631–661. [In Polish with English summary]

Korejwo, K. 1986. Biostratigraphy of the Carboniferous deposits of the Świdnik blocks (Lublin Coal Basin). *Acta Geologica Polonica*, **36** (4), 337–346.

Korejwo, K. and Teller, L. 1968. The Carboniferous of the western part of the Lublin Basin. *Acta Geologica Polonica*, **18** (1), 154–177. [In Polish with English summary]

Korejwo, K. and Teller, L. 1972. The Carboniferous of the Kock elevation. *Acta Geologica Polonica*, **22** (4), 655–675. [In Polish with English summary]

Kostyk, I.O., Matrofailo, M.M., Lelyk, B.I. and Korol, M.D. 2016. New data about sequence formation, compound and capacity of the coal-bearing formation of Carbon of the Lviv-Volyn Basin. *Naukovyi visnik NGU*, **1** (1), 19–31.

Kozłowska, A. and Waksmundzka, M.I. 2020. Diagenesis, sequence stratigraphy and reservoir quality of the Carboniferous deposits of the southeastern Lublin Basin (SE Poland). *Geological Quarterly*, **64** (2), 422–459.

Krassowska, A. (Ed.) 1989. *Profile głębokich otworów wiertniczych Państwowego Instytutu Geologicznego*, **66**, 1–250.

Krzywiec, P. 2007. Tectonics of the Lublin area (SE Poland) – new views based on results of seismic data interpretation. *Biuletyn Państwowego Instytutu Geologicznego*, **422**, 1–18.

Krzywiec, P., Mazur, S., Gągała, Ł., Kufrasa, M., Lewandowski, M., Malinowski, M. and Buffenmyer, V. 2017. Late Carboniferous thin-skinned compressional deformation above the SW Edge of the East European craton as revealed by seismic reflection and potential field data – Correlation with the Variscides and the Appalachians. In: Law, R.D., Thigpen, J.R., Merschat, A.J. and Stowell, H.H. (Eds), Linkages and Feedbacks in Orogenic Systems. *Geological Society of America Memoir*, **213**, 353–372.

Krzywiec, P. and Narkiewicz M., 2003. O stylu strukturalnym kompleksu dewońskokarbońskiego Lubelszczyzny w oparciu o wyniki interpretacji danych sejsmicznych. *Przegląd Geologiczny*, **51** (9), 795–797.

Kufrasa, M., Stypa, A., Krzywiec, P. and Słonka, Ł., 2019. Late Carboniferous thin-skinned deformation in the Lublin Basin, SE Poland: results of combined seismic data interpretation, structural restoration and subsidence analysis. *Annales Societatis Geologorum Poloniae*, **89** (2), 175–194.

Le Maitre, R. W., Bateman, P., Dudek, A., Keller, J., Lameyre, J., Le Bas, M. J., Sabine, P.A., Schmid, R., Sørensen, H., Streckeisen, A., Wooley, A.R. and Zanettin, B. 1989. A classification of ignous rocks and glossary of terms: Recommendations of the International Union of Geological Sciences Subcommision on the Systematic of Ignous Rocks. Blackwell Scientific Publications, Oxford.

Łydka, K. 1996. Diageneza wulkanoklastyków. *Przegląd Geologiczny*, **44** (6), 619–620.

Martinsen, O.J. 1994. Evolution of an incised-valley fill, the Pine Ridge Sandstone of Southeastern Wyoming, U.S.A.: systematic sedimentary response to relative sea-level change, In: Dalrymple, R.W., Boyd, R. and Zaitlin, B.A. (Eds), Incised-valley Systems: Origin and Sedimentary Sequences. *Society of Economic Paleontologists and Mineralogists Special Publication*, **51**, 109–128.

Matyja, H. 2008. Pomeranian basin (NW Poland) and its sedimentary evolution during Mississippian times. *Geological Journal*, **43** (2-3), 123–150.

Mazur, S., Aleksandrowski, P., Kryza, R. and Oberc-Dziedzic T. 2006. The Variscan orogen in Poland. *Geological Quarterly*, **50** (1), 89–119.

Mazur, S., Aleksandrowski, P., Turniak, K., Krzemiński, L., Mastalerz, K., Górecka-Nowak, A., Kurowski, L., Żelaźniewicz, A. and Fanning, M.C. 2010. Uplift and late orogenic deformation of the Central European Variscan belt as revealed by sediment provenance and structural record in the Carboniferous foreland basin of western Poland. *International Journal of Earth Sciences*, **99** (1), 47–64.

Miall, A.D. 1977. A Review of the braided-river depositional environment. *Earth Science Rev*iews, **13** (1), 1–62.

Miall, A.D. 1978. Lithofacies types and vertical profile models in braided river deposits: a summary. In: Miall, A.D. (Ed.), Fluvial sedimentology. *Canadian Society of Petroleum Geologists Memoir*, **5**, 597–604.

Miall, A.D. 1986. Deltas. In: Walker, R.G. (Ed.), Facies Models 2nd Edition, *Geoscience Canada Reprint Series 1*, 105–118.

Miall, A.D. 1996. The Geology of Fluvial Deposits Sedimentary Facies, Basin Analysis, and Petroleum Geology, 26–30; 40–41. Springer; Berlin, Heidelberg.

Michum, Jr R.M. 1977. Seismic Stratigraphy and Global Changes of Sea Level, Part 11: Glossary of Terms used in Seismic Stratigraphy: Section 2. Application of Seismic Reflection Configuration to Stratigraphic Interpretation. In: Payton, E. (Ed) Seismic Stratigraphy – Applications to Hydrocarbon Exploration. *American Association of Petroleum Geologists Memoir*, **26**, 205–212.

Miłaczewski, L. 2010. Subcrop map of the sub-Carboniferous unconformity. In: Modliński Z. (Ed.), Paleogeological Atlas of the sub-Permian Paleozoic of the East-European Craton in Poland and neighbouring areas. PIG-PIB; Warszawa. [In Polish with English summary]

Miłaczewski, L. and Niemczycka, T. 1967. Geological structure of the Niedrzwica region. *Kwartalnik Geologiczny*, **11** (3), 557–571. [In Polish with English summary]

Migier, T. 1988. Macrofloral stratigraphy of the Carboniferous deposits. In: Dembowski, Z. and Porzycki, J. (Eds), Carboniferous of the Lublin Coal Basin. *Prace Instytutu Geologicznego*, **122**, 120–131; 234–235. [In Polish with English summary]

Musiał, Ł. and Tabor, M. 1979. Stratygrafia karbonu Lubelskiego Zagłębia Węglowego na podstawie makrofauny. In: Migier, T. (Ed.), Stratygrafia Węglonośnej Formacji Karbońskiej w Polsce, II Sympozjum Sosnowiec, 4–5 maja 1977, 35–43. Wydawnictwa Geologiczne; Warszawa.

Musiał, Ł. and Tabor, M. 1988. Macrofaunal stratigraphy of Carboniferous. In: Dembowski, Z. and Porzycki, J. (Eds), Carboniferous of the Lublin Coal Basin. *Prace Instytutu*

Geologicznego, **122**, 88–122; 232–233. [In Polish with English summary]

Musiał, Ł. and Tabor, M. 1989. Stratygrafia karbonu na podstawie makrofauny. In: Krassowska, A. (Ed.), *Profile Głębokich Otworów Wiertniczych Państwowego Instytutu Geologicznego*, **66**, 105–108.

Muszyński, A., Biernacka, J., Lorenc, S., Protas, A., Urbanek, Z. and Wojewoda, J. 1996. Petrology and a depositional environment of Lower Carboniferous rocks near Dygowo and Kłanino (the Koszalin-Chojnice zone). *Geologos*, **1**, 93–126. [In Polish with English summary]

Narkiewicz, M. 2007. Development and inversion of Devonian and Carboniferous basins in the eastern part of the Variscan foreland (Poland). *Geological Quarterly*, **51** (3), 231–256.

Narkiewicz, M. 2020. The Variscan foreland in Poland revisited: new data and new concepts. *Geological Quarterly*, **64** (2), 377–401.

Narkiewicz, M., Miłaczewski, L., Krzywiec, P. and Szewczyk, J. 1998. Outline of the Devonian depositional architecture in the Radom-Lublin area. In: Narkiewicz, M. (Ed.), Sedimentary basin analysis of the Polish Lowlands. *Prace Państwowego Instytutu Geologicznego*, **165**, 57–72.

Nemec, W. and Postma, G. 1993. Quaternary alluvial fans in south-western Crete: sedimentation processes and geomorphic evolution. In: Marzo, M. and Puigdefabregas, C. (Eds), Alluvial Sedimentation. *International Association of Sedimentologists, Special Publication*, **17**, 235–276.

Nemec, W. and Steel, R.J. 1984. Alluvial and coastal conglomerates: their significant features and some comments on gravelly mass-flow deposits. In: Koster, E.H. and Steel, R.J. (Eds), Sedimentology of Gravels and Conglomerates. *Canadian Society of Petroleum Geologists Memoir*, **10**, 1–31.

Niemczycka, T. (Ed.) 1978. *Profile Głębokich Otworów Wiertniczych Instytutu Geologicznego*, **45**, 1–292.

Nosova, A.A., Veretennikov, N.V. and Levskii, L.K. 2005. Nature of the mantle source and specific features of crustal contamination of Neoproterozoic flood basalts of the Volhynia Province (Nd-Sr Isotopic and ICP-MS Geochemical Data). *Doklady Earth Sciences*, **401A**, 429–433. Translated from *Doklady Earth Sciences*, **401**, 521–525.

Pańczyk, M. and Nawrocki, J. 2015. Tournaisian $^{40}Ar/^{39}Ar$ age from alkaline basalts from the Lublin Basin (SE Poland). *Geological Quarterly*, **59** (3), 473–478.

Pettijohn, F.J., Potter, P.E. and Siever, R. 1972. Sand and Sandstone, 583 pp. New York, Springer.

Popek, T., 1986. Przejawy wulkanizmu w górnym wizenie na obszarze lubelskim. *Przegląd Geologiczny*, **4**, 212–215.

Porzycki, J. 1979. Litostratygrafia osadów karbonu Lubelskiego Zagłębia Węglowego. In: Migier, T. (Ed.), Stratygrafia węglonośnej formacji karbońskiej w Polsce. II Sympozjum, Sosnowiec, 19–27. Wydawnictwa Geologiczne; Warszawa.

Porzycki, J. 1988. History of geological survey and discovery of the Lublin Coal Basin. Lithologic and sedimentologic characteristics of Carboniferous deposits, In: Dembowski, Z. and Porzycki, J. (Eds), Carboniferous of the Lublin Coal Basin. *Prace Instytutu Geologicznego*, **122**, 9–18; 40–76; 226–227; 229–231. [In Polish with English summary]

Porzycki, J. and Zdanowski, A. 1995. Southeastern Poland (Lublin Carboniferous Basin), In: Zdanowski, A. and Żakowa, H. (Eds), The Carboniferous System in Poland. *Prace Państwowego Instytutu Geologicznego*, **168**, 102–109.

Postma, G. 1990. An analysis of the variation in delta architecture. *Terra Nova*, **2** (2), 124–130.

Posamentier, H.W. and Allen, G.P. 1999. Siliciclastic Sequence Stratigraphy: Concepts and Applications. *Society of Economic Paleontologists and Mineralogists Concepts in Sedimentology and Paleontology*, **7**, 1–210.

Posamentier, H.W., Jervey, M.T. and Vail, P.R. 1988. Eustatic controls on clastic deposition. I – conceptual framework. In: Wilgus, C.K., Hastings, B.S., Kendall, C.G.S.C., Posamentier, H.W., Ross, C.A. and Van Wagoner, J.C. (Eds), Sea-Level Changes: An Integrated Approach. *Society of Economic Paleontologists and Mineralogists Special Publication*, **42**, 110–124.

Porębski, S.J. and Steel R.J. 2003. Shelf-margin deltas: their stratigraphic significance and relation to deepwater sands. *Earth-Science Reviews*, **62**, 283–326.

Pożaryski, W. and Dembowski, Z. 1983. Geological Map of Poland and Neighbouring Countries without Cenozoic, Mesozoic and Permian Deposits. Warszawa, Poland, Geological Instytute, scale 1:1,000,000.

Pulham, A.J. 1989. Controls on internal structure and architecture of sandstone bodies within Upper Carboniferous fluvial-dominated deltas, County Clare, western Ireland. In: Whateley, M.K.G. and Pickering, K.T. (Eds), Deltas: Sites and Traps for Fossil Fuels. *Geological Society Special Publication*, **41**, 179–203.

Ramsbottom, W.H.C. 1977. Major cycles of transgression and regression (mesothems) in the Namurian. *Proceedings of the Yorkshire Geological Society,* **41** (3), 261–291.

Ramsbottom, W.H.C. 1978. Namurian mesothems in South Wales and northern France. *Journal of the Geological Society*, **135** (3), 307–312.

Reading, H.G. 1978. Facies. In: Reading, H.G. (Ed.), Sedimentary Environments and Facies, 4–14. Blackwell Science; Oxford.

Rottella, M. and Simandl, G.J. 2004. Marilla perlite – volcanic glass occurrence, British Columbia, Canada. In: Simandl, G.J., McMillan, W.J. and Robinson, N. (Eds), British Columbia Ministry of Energy Mines and Petroleum Resources, Paper 2004-2, 265–272. Geological Survey Branch; Victoria.

Rust, B.R. 1978. A classification of alluvial channel systems. In: Miall, A.D. (Ed.), Fluvial Sedimentology. *Canadian Society of Petroleum Geologists Memoir*, **5**, 187–198.

Ryka, W. and Maliszewska, A. (Eds) 1991. Słownik petrograficzny. II wyd., 415 pp. Wydawnictwa Geologiczne; Warszawa.

Scruton, P.C. 1960. Delta building and the deltaic sequence. In:

Shepard, F.P., Phleger, F.B. and Angel, T.H. (Eds), Recent sediments, northwest Gulf of Mexico, 82–102. American Association of Petroleum Geologists Special Publication; Tulsa.

Segerstrom, K. 1950. Erosion studies of Paricutin, State of Michoacan, Mexico. U. S. *Geological Survey Bulletin*, **965-A**, 1–164.

Shulga, V.F., Zdanovski, A., Zayceva, L.B., Yvanova, A.V., Yvanyna, A.V., Korol, N.D., Kotasova, A., Kotas, A., Kostyk, I.O., Lelyk, B.I., Migier, T., Manycev, B.Y., Matrofailo, M.M., Ptak, B., Savcuk, V.S., Sedayeva, G.M. and Stepanenko, J.G. 2007. Correlation of the Carboniferous coal-bearing formations of the Lviv-Volyn and Lublin Basins, 428 pp. National Academy of Sciences of Ukraine Institute of Geological Sciences Polish State Geological Institute Upper Silesian Branch; Kiev. [In Russian with English and Polish summaries]

Shumlyanskyy, L.V. 2014. Geochemistry of the Osnisk-Mikashevichy Volcanoplutonic Complex of the Ukrainian Shield. *Geochemistry International*, **52** (11), 912–924.

Siemaszko, E. 1978. Permian effusive rocks from SW part of the Fore-Sudetic Monocline. *Kwartalnik Geologiczny*, **22** (3), 571–590. [In Polish with English summary]

Skompski S. 1988. Limestone microfacies and facies position of Upper Visean sediments in north-eastern part of the Lublin Coal Basin. *Przegląd Geologiczny*, **36** (1), 25–30. [In Polish with English summary]

Skompski, S. 1995. Succession of limestone microfacies as a key to the origin of the Yoredale-type cyclicity (Viséan/Namurian, Lublin Basin, Poland). XIII International Congress Carboniferous–Permian, Kraków, Abstracts, 133.

Skompski, S. 1996. Stratigraphic position and facies significance of the limestone bands in the subsurface Carboniferous succession of the Lublin Upland. *Acta Geologica Polonica*, **46** (3), 171–268.

Skompski, S. 1998. Regional and global chronostratigraphic correlation levels in the late Visean to Westphalian succession of the Lublin Basin (SE Poland). *Geological Quarterly*, **42**, 121–130.

Skompski, S. 2011. Wykształcenie facjalne wapieni dolnokarbońskich w rejonie otworu Parczew IG 10. In: Pacześna, J. (Ed.), *Profile Głębokich Otworów Wiertniczych Państwowego Instytutu Geologicznego*, **130**, 111–116. [In Polish with English summary]

Skompski, S. and Soboń-Podgórska, J. 1980. Foraminifers and conodonts in the Viséan deposits of the Lublin Upland. *Acta Geologica Polonica*, **30**, 87–96.

Smith, D.G. 1983. Anastomosed fluvial deposits: modern examples from Western Canada. In: Collinson, J. and Lewin, J. (Eds), Modern and Ancient Fluvial Systems. *Special Publication of the International Association of Sedimentologists*, **6**, 155–168.

Soboń-Podgórska, J. 1988. Microfaunal stratigraphy of the Carboniferous deposits (foraminifers). In: Dembowski, Z. and Porzycki, J. (Eds), Carboniferous of the Lublin Coal Basin. *Prace Instytutu Geologicznego*, **122**, 112–120; 233–234. [In Polish with English summary]

Soboń-Podgórska, J. and Tomaś, A. 1995. Foraminifera. In: Zdanowski, A. and Żakowa, H. (Eds), The Carboniferous System in Poland. *Prace Państwowego Instytutu Geologicznego*, **148**, 44–47.

Svendsen, J., Stollhofen, H., Krapf, C.B.E. and Stanistreet, I.G. 2003. Mass and hyperconcentrated flow deposits record dune damming and catastrophic breakthrough of ephemeral rivers, Skeleton Coast Erg, Namibia. *Sedimentary Geology*, **160** (1-3), 7–31.

Szulczewski, M., Bełka, Z. and Skompski, S. 1996. The drowning of carbonate platform: an example from the Devonian–Carboniferous of the southwestern Holy Cross Mountains, Poland. *Sedimentary Geology*, **106** (1-2), 21–49.

Środoń, J., Paszkowski, M., Drygant, D., Anczkiewicz, A. and Banaś, M. 2013. Thermal history of Lower Paleozoic rocks on the Peri-Tornquist margin of the East European Craton (Podolia, Ukraine) inferred from combined XRD, K-Ar, and AFT data. *Clays and Clay Minerals*, **61** (2), 107–132.

Tomaszczyk, M. and Jarosiński, M. 2017. The Kock Fault Zone as an indicator of tectonic stress regime changes at the margin of the East European Craton (Poland). *Geological Quarterly*, **61**, 908–925.

Tunbridge, I.P. 1981. Sandy high-energy flood sedimentation – some criteria for recognition, with an example from the Devonian of SW England. *Sedimentary Geology*, **28** (2), 79–95.

Turner, B.R. and Whateley, M.K.G. 1983. Structural and sedimentological controls of coal deposition in the Nongoma graben, northern Zululand, South Africa. In: Collinson, J.D. and Lewin, J. (Eds), Modern and ancient fluvial systems. *Special Publication of the International Association of Sedimentologists*, **6**, 457–471.

Vail, P.R., Todd, R.G. 1981. Northern North Sea Jurassic unconformities, chronostratigraphy and sea-level changes from seismic stratigraphy. In: Illing, L.V. and Hobson, G.D. (Eds), Petroleum Geology of the Continental Shelf of North West Europe, 216–235. Heyden and Son Ltd.; London.

VanWagoner, J.C. 1985. Reservoir facies distribution as controlled by sea-level change. Society of Economic Paleontologists and Mineralogists Mid-Year Meeting Abstracts, Golden, Colorado, August 11–14, 91–92. Society of Economic Paleontologists and Mineralogists; Tulsa.

Van Wagoner, J.C., Posamentier, H.W., Mitchum, R.M. Jr, Vail, P.R., Sarg, J.F., Loutit, T.S. and Hardenbol, J. 1988. An overview of the fundamentals of sequence stratigraphy and key definitions. In: Wilgus, K., Hastings, B.S., Kendall, C.G.St.C., Posamentier, H.W., Ross, C.A. and Van Wagoner, J.C. (Eds), Sea-Level Changes – An Integrated Approach. *Society of Economic Paleontologists and Mineralogists Special Publication*, **42**, 39–45.

Waksmundzka, M.I. 1998. Depositional architecture of the

Carboniferous Lublin Basin. In: Narkiewicz, M. (Ed.), Sedimentary basin analysis of the Polish Lowlands. *Prace Państwowego Instytutu Geologicznego*, **165**, 89–100. [In Polish with English summary]

Waksmundzka, M.I. 2007. Karbon. Litologia, stratygrafia i sedymentologia. In: Pacześna, J. (Ed.), *Profile Głębokich Otworów Wiertniczych Państwowego Instytutu Geologicznego*, **118**, 124–130. [In Polish with English summary]

Waksmundzka, M.I. 2008. Correlation and origin of the Carboniferous sandstones in the light of sequence stratigraphy and their hydrocarbon potential in the NW and Central parts of the Lublin Basin. *Biuletyn Państwowego Instytutu Geologicznego*, **429**, 215–224. [In Polish with English summary]

Waksmundzka, M.I. 2010a. Sequence stratigraphy of Carboniferous paralic deposits in the Lublin Basin (SE Poland). *Acta Geologica Polonica*, **60** (4), 557–597.

Waksmundzka, M.I. 2010b. Lithofacies-paleothickness and worm's eye maps of Carboniferous. Plates 21–24, 33–35. In: Modliński, Z. (Ed.), Paleogeological Atlas of the sub-Permian Paleozoic of the East-European Craton in Poland and neighbouring areas. PIG-PIB Warszawa. [In Polish with English summary]

Waksmundzka, M.I. 2011. Karbon. Litologia, sedymentologia i stratygrafia. In: Pacześna, J. (Ed.), *Profile Głębokich Otworów Wiertniczych Państwowego Instytutu Geologicznego*, **130**, 101–108. [In Polish with English summary]

Waksmundzka, M.I. 2012. Braided-river and hyperconcentrated-flow deposits from the Carboniferous of the Lublin Basin (SE Poland) – a sedimentological study of core data. *Geologos*, **18** (3), 135–161.

Waksmundzka, M.I. 2013. Carboniferous coarsening-upward and non-gradational cyclothems in the Lublin Basin (SE Poland): palaeoclimatic implications. In: Gąsiewicz, A. and Słowakiewicz, M. (Eds), Palaeozoic Climate Cycles: Their Evolutionary and Sedimentological Impact. *Geological Society, London, Special Publications*, **376**, 141–175.

Waksmundzka, M.I. and Buła, Z. 2020. Geological Map of Poland without Cenozoic, Mesozoic and Permian deposits 1:2,5000,000. In: Nawrocki, J. and Becker, A. (Eds), Geological Atlas of Poland, 28–29. PIG-PIB; Warszawa.

Walker, R.G. 1992. Facies, facies models, and modern stratigraphic concepts. In: Walker, R.G. and James, N.P. (Eds), Facies Models: Response to Sea Level Change, 1–14. Geological Association of Canada; St. John's.

Walker, G.P.L. 1973. Lengths of lava flows. *Philosophical Transactions of the Royal Society London*, **274** (1238), 107–118.

Winchester, J.A. and Floyd, P.A. 1977. Geochemical discrimination of different magma series and their differentiation products using immobile elements. *Chemical Geology*, **20**, 325–343.

Wiszniewska, J. and Tołkanowicz, E. 2015. Raw rock resources of the Volhynia Province during the period of Second Republic of Poland and their utilization. *Przegląd Geologiczny*, **63** (9), 525–530. [In Polish with English summary]

Woszczyńska, S. 2011. The Carboniferous micropalaeontology based on Foraminifera and Ostracoda. In: Pacześna, J. (Ed.), *Profile Głębokich Otworów Wiertniczych Państwowego Instytutu Geologicznego*, **130**, 109–110. [In Polish with English summary]

Wright, L.D. 1977. Sediment transport and deposition at river mouths: a synthesis. *Geological Society of America Bulletin*, **88** (6), 857–868.

Wright, LD. and Coleman, J.M. 1974. Mississippi river mouth processes: effluent dynamics and morphologic development. *Journal of Geology*, **82** (6), 751–778.

Zieliński, T. 1992a. Marginal moraines of NE Poland – sediments and depositional conditions. *Prace Naukowe Uniwersytetu Śląskiego*, **1325**, 7–95.

Zieliński, T. 1992b. Proglacial valleys facies of the Silesian Upland – genetic factors and their sedimentological effects. *Geologia Sudetica*, **26** (1–170), 83–118.

Zieliński, T. 1995. Kod litofacjalny i litogenetyczny – konstrukcja i zastosowanie. In: Mycielska-Dowgiałło, E. and Rutkowski, J. (Eds), Badania osadów czwartorzędowych, Wybrane metody i interpretacja wyników, 220–235. Uniwersytet Warszawski; Warszawa.

Zieliński, T. 2015. Sedymentologia. Osady rzek i jezior, 594 pp. Wydawnictwo Naukowe UAM; Poznań.

Żelichowski, A.M. 1969. Karbon. In: Depowski, S. (Ed.), Ropo- i gazonośność obszaru lubelskiego na tle budowy geologicznej – część I: Budowa geologiczna obszaru lubelskiego. *Prace Geostrukturalne Instytutu Geologicznego*, 70–85.

Żelichowski, A.M. 1972. Evolution of the geological structure of the area between the Góry Świętokrzyskie and the River Bug. *Biuletyn Instytutu Geologicznego*, **263**, 7–97; 91–97. [In Polish with English summary]

Żelichowski, A.M. 1987. Development of the Carboniferous of the SW margin of the East European Platform in Poland. *Przegląd Geologiczny*, **35** (5), 230–237. [In Polish with English summary]

Żelichowski, A.M. and Kozłowski, S. (Eds) 1983. Atlas of geological structure and mineral deposits in the Lublin region. Wydawnictwa Geologiczne; Warszawa. [In Polish with English summary]

Żelichowski, A.M., Porzycki, J., Cebulak, S., Musiał, Ł., Tabor, M., Migier, T. and Waksmundzka, M.I. 2011. Profil litologiczno-stratygraficzny Karbon. In: Pacześna, J. (Ed.), *Profile Głębokich Otworów Wiertniczych Państwowego Instytutu Geologicznego*, **130**, 20–39. [In Polish with English summary]

Manuscript submitted: 6th August 2020
Revised version accepted: 20th November 2020